

# Stabilizing Rate of Stochastic Control Systems

Hui Jia\*

Yuan-Hua Ni†

Guangchen Wang‡

December 15, 2025

## Abstract

This paper develops a quantitative framework for analyzing the mean-square exponential stabilization of stochastic linear systems with multiplicative noise, focusing specifically on the optimal stabilizing rate, which characterizes the fastest exponential stabilization achievable under admissible control policies. Our contributions are twofold. First, we extend the norm-based techniques from deterministic switched systems to the stochastic setting, deriving a verifiable necessary and sufficient condition for the exact attainability of the optimal stabilizing rate, together with computable upper and lower bounds. Second, by restricting attention to state-feedback policies, we reformulate the optimal stabilizing rate problem as an optimal control problem with a nonlinear cost functional and derive a Bellman-type equation. Since this Bellman-type equation is not directly tractable, we recast it as a nonlinear matrix eigenvalue problem whose valid solutions require strictly positive-definite matrices. To ensure the existence of such solutions, we introduce a regularization scheme and develop a Regularized Normalized Value Iteration (RNDI) algorithm, which in turn converges to strictly positive-definite fixed points for a perturbed version of the original nonlinear matrix eigenvalue problem while producing feedback controllers. Evaluating these regularized solutions further yields certified lower and upper bounds for the optimal stabilizing rate, resulting in a constructive and verifiable framework for determining the fastest achievable mean-square stabilization under multiplicative noise.

**Keywords:** stochastic control, mean-square exponential stability, multiplicative noise, stabilizing rate, optimal feedback control, regularization.

## 1 Introduction

In the theoretical framework of stochastic control, stabilizability analysis remains a core topic that permeates both fundamental research and engineering applications; classic theories focus centrally on a pivotal question for uncertain, noisy dynamic systems: can controller design guarantee bounded and asymptotically convergent trajectories? Classic results (e.g., [H. J. Kushner \(1967\)](#)) based on Lyapunov methods and Riccati theory provide affirmative answers under appropriate conditions. However, as modern engineering systems grow increasingly complex, merely proving stabilizability is no longer sufficient; the rate of stabilization, meaning how fast the state returns to the desired equilibrium, has become equally critical. This quantitative aspect directly influences both safety and performance in practical scenarios. For instance, in power and energy systems ([Zhang and Cortés \(2019\)](#); [Weitenberg et al. \(2018\)](#)), distributed frequency control has been shown to achieve exponential convergence and to examine how communication disruptions influence the resulting convergence rate, while transient

\*College of Artificial Intelligence, Nankai University, Tianjin 300350, P.R. China, E-mail: 2120210368@mail.nankai.edu.cn

†Corresponding author. College of Artificial Intelligence, Nankai University, Tianjin 300350, P.R. China, E-mail: yhni@nankai.edu.cn

‡School of Control Science and Engineering, Shandong University, Jinan 250061, P.R. China, E-mail: wguangchen@sdu.edu.cn

frequency control enforces finite time return to a prescribed safe band with a guaranteed convergence rate, and thus the pace of recovery is treated as part of the design rather than a byproduct. For robotics and other safety-critical infrastructures (Ames et al.; Nguyen and Sreenath (2016)), control Lyapunov and control barrier function methods often operate in tandem to enforce both stability and safety, and in particular, exponential barrier formulations embed explicit requirements on how rapidly safety constraints must be restored, indicating that the rate of convergence is an inherent component of reliable operation. Across these domains, stabilization feasibility alone is insufficient and one must also take into account how rapidly stability is achieved.

Over the past decades, the classic theory of stability in deterministic systems is well established and provides the foundation for much of modern control. Lyapunov's second method (Khalil and Grizzle (2002)) offers general certificates of asymptotic and exponential stability for nonlinear systems, while for linear time-invariant systems, algebraic Riccati equations and linear quadratic regulator (LQR) design yield constructive stabilizing state-feedback laws (Anderson and Moore (1971)). The development of linear matrix inequality (LMI) technique (Boyd et al. (1994)) unifies and generalizes classic criteria, making stability analysis and controller synthesis numerically tractable. These methods constitute a mature toolbox: Lyapunov theory provides the conceptual basis, Riccati and LQR methods furnish constructive synthesis, and LMIs deliver computational scalability. Yet, all of these are primarily designed to decide whether stabilization is feasible and they rarely provide certified information about the *rate* of stabilization. When stochastic disturbances are present, the problem becomes significantly more challenging. In particular, systems with *multiplicative noise*, where randomness enters directly through system coefficients, arise naturally in applications ranging from portfolio optimization (Dom-brovskii and Lyashenko (2003)) to systems biology (Yao et al. (2011)). For such systems, the standard notion is *mean-square exponential stability* (ESMS), which requires the second moment of the state to decay exponentially. This problem has been studied for decades, with early contributions dating back to the late 1960s (Kleinman (1969); McLane (1969); Wonham (1967)) and the continued development through numerous works Zhang et al. (2015); Feng et al. (2018a); Qi and Zhang (2018); Feng et al. (2018b); Li et al. (2021). Much of this literature establishes stability conditions via modified algebraic Riccati equations (Wonham (1967); Jacques and Jan (1976); Blankenship (1977)) or LMI formulations (Boyd et al. (1994); Elia (2005)), thereby connecting mean-square stability analysis to convex optimization. In parallel, a frequency-domain viewpoint is initiated by Willems and Blankenship (1971), who establish necessary and sufficient conditions for mean-square stability in single-input single-output systems; this perspective has since been extended to multi-input multi-output cases (Hinrichsen and Pritchard (1996); Lu and Skelton (2002); Qi et al. (2017); Bamieh and Filo (2020)). From this standpoint, mean-square stability can be interpreted as a robust stability problem with respect to stochastic uncertainties. These approaches are powerful and constructive, but they remain *qualitative*: they tell us whether stabilization is possible, not how fast it can be achieved.

A complementary quantitative perspective is introduced by Hu et al. (2017), who quantifies stabilization both by feasibility and by how fast it can be achieved. For deterministic switched systems, this framework enables computable upper and lower bounds on the fastest achievable stabilizing rate through norm and seminorm based constructions (Hu et al. (2017, 2024)). These results establish a foundation for quantitative stability analysis, but they rely on finite-dimensional properties, such as norm equivalence. These properties fail in stochastic settings, where the natural state space is infinite-dimensional and none of the finite-dimensional assumptions carry over. Consequently, despite the appeal of Hu's quantitative perspective, a systematic extension to stochastic settings remains open.

To sum up, several important limitations remain in the existing literature. First, studies on stochastic systems with multiplicative noise provide tractable feasibility conditions, but they seldom address how fast such systems can be stabilized in the mean-square sense. Second, works on deterministic switched systems do quantify the fastest convergence rate, yet their methods rely critically on finite-dimensional properties that are absent in the stochastic setting. Third, there remains no unified framework that can offer a computable and verifiable characterization of fastest stabilizing rate

for stochastic systems with multiplicative disturbances. To bridge these gaps, this paper develops a unified framework for quantifying the *optimal stabilizing rate*, defined as the fastest mean-square exponential stabilization achievable under admissible control policies for stochastic systems with multiplicative noise. We first extend the norm-based approach of deterministic switched systems (Hu et al. (2017)) to the stochastic setting, thereby generalizing the quantitative notion of stabilization to random environments. Second, and more importantly, restricting to state-feedback policies, we reformulate the determination of fastest stabilizing rate as an optimal control problem with a nonlinear cost functional. Building on this formulation, we propose the Regularized Normalized Value Iteration (RNNVI) algorithm to compute the certified upper and lower bounds for the fastest stabilizing rate under state-feedback control policies. The main contributions are summarized as follows.

### 1. Norm-based characterization of the optimal stabilizing rate

We extend the norm-based framework of Hu et al. (2017) to stochastic systems with multiplicative noise, providing necessary and sufficient condition for the attainability and upper/lower bounds for the optimal stabilizing rate.

This extension is technically nontrivial: norms on the infinite-dimensional space  $L^2(\Omega; \mathbb{R}^n)$  are no longer equivalent. We establish some norm equivalence under suitable conditions and obtain a rigorous norm-based characterization in the stochastic setting.

### 2. Bridging stabilization theory and optimal control

Restricting to state-feedback policies, we reformulate the optimal stabilizing rate problem as an *optimal control problem with a nonlinear cost functional* and derive a *Bellman-type equation*. As this equation is not directly amenable to analysis, it is reduced to a nonlinear matrix eigenvalue problem that requires a strictly positive-definite solution, providing a tractable representation for determining the optimal stabilizing rate.

### 3. Regularized approximation for nonlinear matrix eigenvalue problems

The nonlinear matrix eigenvalue equation derived from the Bellman-type formulation may fail to admit strictly positive-definite solutions, leading to ill-posedness on the boundary of the semi-definite cone. To address this puzzle, we introduce a regularization parameter, which guarantees the existence of a strictly positive-definite fixed point.

More generally, this procedure offers a regularized approximation approach for such nonlinear matrix eigenvalue problems that require positive-definite solutions. The resulting formulation not only restores well-posedness but also offers a constructive pathway to approximate eigen-solutions in settings where direct solutions are otherwise unattainable.

### 4. Regularized Normalized Value Iteration providing certified bounds for the optimal stabilizing rate

To make this regularized approach constructive, we develop the RNNVI algorithm. RNNVI iteratively computes the positive-definite solutions and the corresponding feedback controllers for a sequence of decreasing regularization parameters. The procedure starts from a relatively large value of the regularization parameter, for which the convergence is numerically reliable, and proceeds gradually through a continuation scheme that uses each computed solution as the initialization for the next stage. Each iteration provides verifiable upper and lower bounds for the optimal stabilizing rate under state-feedback control policies, and the tightest bounds obtain over all parameter values are reported as the final certified estimate.

Together, these results provide both theoretical guarantees and computational tools for analyzing and quantifying the stochastic optimal stabilizing rate.

The remainder of the paper is organized as follows. Section 2 introduces the stochastic system model and the definition of the optimal stabilizing rate. Section 3 extends the norm-based framework

of [Hu et al. \(2017\)](#) to our stochastic setting. Section 4 reformulates the problem as an optimal control problem and derives a Bellman-type equation, which is shown to reduce to a nonlinear matrix eigenvalue equation. Section 5 develops the RVI algorithm to obtain bounds for the optimal stabilizing rate. Section 6 reports numerical experiments that illustrate the performance of the proposed method. Section 7 then concludes this paper.

**Notations.** Let  $\mathbb{E}[\cdot]$  denote the mathematical expectation, and  $\mathbb{E}[\cdot \mid \mathcal{F}]$  the conditional expectation with respect to  $\sigma$ -algebra  $\mathcal{F}$ .  $\mathbb{R}_+$  stands for the set of positive real numbers, and  $\mathbb{N}$  represents the set of non-negative integers  $\{0, 1, 2, \dots\}$ . The symbol  $\times$  denotes the Cartesian product of sets.  $\mathbb{S}_+^n$  and  $\mathbb{S}_{++}^n$  denote the sets of  $n \times n$  symmetric positive semi-definite matrices and symmetric positive-definite matrices, respectively; accordingly,  $A \succeq 0$  ( $A \succ 0$ ) indicates that matrix  $A$  is symmetric positive semi-definite (symmetric positive-definite).  $\lambda_{\min}(A)$  and  $\lambda_{\max}(A)$  denote the minimum and maximum eigenvalues of the symmetric matrix  $A$ , respectively. The transpose and inverse of a matrix are denoted by  $(\cdot)^\top$  and  $(\cdot)^{-1}$ , respectively.  $\text{Tr}(A)$  denotes the trace of matrix  $A$ .  $I$  denotes the identity matrix with compatible dimensions, and  $\sigma(x)$  represents the  $\sigma$ -algebra generated by the random variable  $x$ . For a matrix  $A$ ,  $\|A\|$  and  $\|A\|_F$  denote its spectral norm and Frobenius norm, respectively. The infimum of a function  $f$  is denoted as  $f^*$ .  $x \mapsto f(x)$  indicates the mapping from input  $x$  to output  $f(x)$ . For a mapping  $f$ ,  $Df(x)[H]$  denotes directional derivative of  $f$  at  $x$  in direction  $H$  and  $Df(x)$  denotes the corresponding linear operator  $H \mapsto Df(x)[H]$ . Finally,  $L^2(\Omega; \mathbb{R}^m)$  denotes the Hilbert space of  $\mathbb{R}^m$ -valued square-integrable random variables, equipped with the inner product  $\langle x, y \rangle := \mathbb{E}[x^\top y]$  and the induced norm  $(\mathbb{E}[x^\top x])^{1/2}$ .

## 2 Problem Formulation

Consider a discrete-time plant, which evolves according to some discrete-time stochastic difference equation

$$x_{k+1} = (A + \bar{A}\omega_k)x_k + (B + \bar{B}\omega_k)u_k, \quad k \in \mathbb{N}. \quad (1)$$

Here,  $x_k \in \mathbb{R}^n$  and  $u_k \in \mathbb{R}^m$  are the system state and control input, respectively. We assume that the initial state  $x_0$  is Gaussian with mean  $\bar{x}_0$  and covariance  $\Sigma_{\text{init}}$ . The noise sequence  $\{\omega_k\}$  consists of independent and identically distributed (i.i.d) Gaussian random variables with zero mean and variance  $\sigma^2$ , and is assumed independent of  $x_0$ .

Let  $\mathcal{F}_k = \sigma(x_0, \omega_0, \dots, \omega_{k-1})$  be the natural filtration generated by the past information. The control must satisfy the causality constraint that  $u_k$  is  $\mathcal{F}_k$ -measurable, together with a finite-energy condition. Accordingly, we introduce the following admissible control set

$$\mathcal{U} := \{u = (u_0, u_1, \dots) \mid u_k \text{ is } \mathcal{F}_k\text{-measurable, } \mathbb{E}[u_k^\top u_k] < \infty\}.$$

We next introduce some basic notions of mean-square stability.

**Definition 1.** *The control-free system (1) with  $u_k \equiv 0$  is said to be  $\ell^2$ -exponentially mean-square stable, if for any initial value  $x_0$  there exist constants  $\kappa \geq 0$ ,  $\rho \in [0, 1)$  such that the solution of (1) satisfies*

$$\mathbb{E}[x_k^\top x_k] \leq \kappa \rho^{2k} \mathbb{E}[x_0^\top x_0], \quad \forall k \in \mathbb{N}. \quad (2)$$

**Definition 2.** *System (1) is said to be open-loop  $\ell^2$ -exponentially stabilizable in the mean-square sense, if for any initial value  $x_0$ , there exists  $u \in \mathcal{U}$  such that the solution of (1) satisfies (2).*

**Definition 3.** *System (1) is said to be closed-loop  $\ell^2$ -exponentially stabilizable in the mean-square sense, if there exists  $u_k = -Kx_k$  with constant matrices  $K$ , such that for any  $x_0$  the closed-loop system of (1) is  $\ell^2$ -exponentially mean-square stable.*

For linear stochastic system (1), Ni et al. (2015) shows that open-loop  $\ell^2$ -stabilizable is equivalent to closed-loop  $\ell^2$ -stabilizable. Hence, the open-loop  $\ell^2$ -stabilizability and the closed-loop  $\ell^2$ -stabilizability will be both called  $\ell^2$ -stabilizability. Inspired by the work of Hu et al. (2017), where the concept of the *optimal stabilizing rate* is introduced for deterministic switched systems, we extend this concept to the stochastic systems with multiplicative noise. This motivates the following definitions.

**Definition 4.** For each admissible control policy  $u \in \mathcal{U}$ , its mean-square stabilizing rate is defined as

$$\rho(u) := \inf \left\{ \rho \geq 0 \mid \exists \kappa \geq 0 \text{ such that } \mathbb{E}[x_k^\top x_k] \leq \kappa \rho^{2k} \mathbb{E}[x_0^\top x_0], \forall x_0 \in \mathbb{R}^n, \forall k \in \mathbb{N} \right\},$$

where  $\{x_k\}$  denotes the state trajectory of system (1) driven by  $u$ .

It is worth emphasizing that we do *not* assume a priori that system (1) is  $\ell^2$ -exponentially stabilizable in the mean-square sense. The quantity  $\rho(u)$  defined above simply quantifies the exponential rate associated with the chosen admissible control policy  $u$ ; if  $\rho(u) < 1$ , the corresponding state trajectories converge in the mean-square sense, whereas  $\rho(u) \geq 1$  indicates that the mean-square state fails to converge and may instead diverge under this control policy.

**Definition 5.** The optimal stabilizing rate of system (1) is then defined as

$$\rho^* := \inf_{u \in \mathcal{U}} \rho(u),$$

where  $\rho(u)$  denotes the mean-square stabilizing rate of policy  $u$  introduced in Definition 4. A control policy  $u^* \in \mathcal{U}$  (if it exists) is called optimal if it achieves this infimum, i.e.,  $\rho(u^*) = \rho^*$ .

**Remark.** Both  $\rho(u)$  and  $\rho^*$  are always well-defined. Indeed, for any admissible policy  $u \in \mathcal{U}$ , the set

$$\left\{ \rho \geq 0 \mid \exists \kappa \geq 0 : \mathbb{E}[x_k^\top x_k] \leq \kappa \rho^{2k} \mathbb{E}[x_0^\top x_0], \forall x_0 \in \mathbb{R}^n, \forall k \in \mathbb{N} \right\}$$

is nonempty and is bounded below by 0; hence, its infimum  $\rho(u)$  always exists. Since  $\rho^* = \inf_{u \in \mathcal{U}} \rho(u)$  is the infimum of a nonempty set bounded below by 0,  $\rho^*$  also exists. Our definition differs slightly from the deterministic setting of Hu et al. (2017). In Hu et al. (2017), the analogue of the growth inequality  $\|x_k\| \leq \kappa \rho^k \|x_0\|$  used to define the stabilizing rate is written with an arbitrary vector norm on  $\mathbb{R}^n$ ; in finite-dimensional deterministic systems, all norms are equivalent and the stabilizing rate is therefore independent of the chosen norm. For the stochastic system (1), the state evolves in  $L^2(\Omega; \mathbb{R}^n)$ , where different norms are not equivalent in general. Consequently, the value of  $\rho^*$  depends on the chosen norm. This paper works with the mean-square norm  $(\mathbb{E}[x^\top x])^{1/2}$ .

Having introduced the quantities  $\rho(u)$  and  $\rho^*$ , we now state the optimization problem that will serve as the primary object of this paper.

**Problem (OSR).** Solve the optimization problem:

$$\inf_{u \in \mathcal{U}} \rho(u),$$

subject to

$$\begin{cases} x_{k+1} = (A + \bar{A}\omega_k)x_k + (B + \bar{B}\omega_k)u_k, \\ \mathbb{E}[x_k^\top x_k] \leq \kappa \rho^{2k} \mathbb{E}[x_0^\top x_0], \forall k \in \mathbb{N}. \end{cases}$$

**Remark.** The constant  $\kappa$  in Definition 4 does not affect the value of  $\rho(u)$  or  $\rho^*$ . The reason is that  $\kappa$  only compensates for a finite number of initial steps, while  $\rho(u)$  characterizes the asymptotic growth of the second moment as  $k \rightarrow \infty$ . Thus, the optimal stabilizing rate is determined solely by the tail behavior of the system, and not by the particular choice of  $\kappa$ .

**Remark.** Problem (OSR) does not assume mean-square stabilizability. By Definition 5,  $\rho^*$  is the infimum over nonnegative  $\rho$  for which condition stable holds for some  $\kappa$  and an admissible control policy. Accordingly,  $\rho^*$  may be less than, equal to, or greater than one;  $\rho^* < 1$  implies that mean-square stabilization is achievable and  $\rho^*$  characterizes the fastest rate of convergence, whereas  $\rho^* \geq 1$  indicates that only a minimal growth rate can be attained. Throughout this paper, we uniformly refer to  $\rho^*$  as the optimal stabilizing rate.

In the remainder of the paper, we develop two complementary approaches to address Problem (OSR). The first extends the norm-based framework of [Hu et al. \(2017\)](#) to the stochastic setting, yielding a characterization of the optimal stabilizing rate and its computable bounds. The second reformulates the problem as an optimal control problem and leads to a Bellman-type equation. This Bellman equation can be further reduced to a nonlinear matrix eigenvalue problem, which becomes the basis of the RNNI scheme used to approximate  $\rho^*$  and sharpen its computable bounds.

### 3 Norm-Based Characterization of the Optimal Stabilizing Rate

The norm-based framework introduced in [Hu et al. \(2017\)](#) provides a rigorous foundation for analyzing deterministic switched systems, establishing two key results: (i) sufficient conditions for the *exact attainability* of the optimal stabilizing rate, and (ii) computable *upper and lower bounds* for this rate. Our goal in this section is to extend this analytical framework to stochastic system (1).

Unlike the deterministic case, the stochastic setting introduces fundamental analytical obstacles. System state  $x_k$  is a random variable, so the natural state space  $L^2(\Omega; \mathbb{R}^n)$  is infinite-dimensional. Consequently, the standard finite-dimensional equivalence of norms in [Hu et al. \(2017\)](#) no longer holds automatically in this setting. To address this issue, we impose a necessary and sufficient condition that restores *norm equivalence* on  $L^2(\Omega; \mathbb{R}^n)$ . To this end, let the mean-square norm be defined as

$$\|x\|_{\text{ms}} := (\mathbb{E}[x^\top x])^{1/2}.$$

By Definition 5, the case  $\rho^* = 0$  would mean that, for any rate  $\rho > 0$ , there exists a policy  $u \in \mathcal{U}$  and a constant  $\kappa$  such that

$$\mathbb{E}[x_k^\top x_k] \leq \kappa \rho^{2k} \mathbb{E}[x_0^\top x_0], \quad \forall k \in \mathbb{N},$$

that is, arbitrarily fast mean-square exponential stabilization is possible. Such behavior is highly degenerate and not of interest in this work, so we focus on the nontrivial case and assume  $\rho^* > 0$  in the sequel. Following the construction in [Hu et al. \(2017\)](#), for each initial condition  $x_0 \in L^2(\Omega; \mathbb{R}^n)$ , define the extended real-valued functional

$$\eta(x_0) := \inf_{u \in \mathcal{U}} \sup_{k \in \mathbb{N}} \frac{\|x_k\|_{\text{ms}}}{(\rho^*)^k}, \quad (3)$$

where state trajectory  $x_k$  evolves according to (1) under control policy  $u$ . We then introduce the domain of finiteness

$$\mathcal{W} := \{x \in L^2(\Omega; \mathbb{R}^n) \mid \eta(x) < \infty\}.$$

**Lemma 1.** Suppose  $\mathcal{W} = L^2(\Omega; \mathbb{R}^n)$ . Then, the mapping  $\eta : L^2(\Omega; \mathbb{R}^n) \rightarrow [0, \infty)$  defined by (3) is a norm on  $L^2(\Omega; \mathbb{R}^n)$ .

*Proof.* For  $(x_0, u) \in L^2(\Omega; \mathbb{R}^n) \times \mathcal{U}$ , define

$$F(x_0, u) := \sup_{k \in \mathbb{N}} \frac{\|x_k\|_{\text{ms}}}{(\rho^*)^k}, \quad \eta(x_0) = \inf_{u \in \mathcal{U}} F(x_0, u).$$

We first establish the positive definiteness. For any  $x_0$  and  $u \in \mathcal{U}$ ,  $\|x_k\|_{\text{ms}} \geq 0$  implies  $F(x_0, u) \geq 0$  and hence  $\eta(x_0) \geq 0$ . If  $x_0 = 0$ , choosing  $u \equiv 0$  yields  $x_k \equiv 0$  for all  $k$ , and thus  $\eta(0) = 0$ . Conversely, if  $x_0 \neq 0$ , then the term with  $k = 0$  gives  $F(x_0, u) \geq \|x_0\|_{\text{ms}} > 0$  for all  $u$ , and thus  $\eta(x_0) > 0$ .

By the linearity of the dynamics, we have  $F(\alpha x_0, \alpha u) = \alpha F(x_0, u)$  for  $\alpha > 0$ . Since  $\alpha u \in \mathcal{U}$ , this fact implies  $\eta(\alpha x_0) = \alpha \eta(x_0)$ . Take  $x_0^{(1)}, x_0^{(2)} \in L^2(\Omega; \mathbb{R}^n)$  and  $u^{(1)}, u^{(2)} \in \mathcal{U}$ . By the convexity of  $\mathcal{U}$  and the Minkowskis inequality, we obtain

$$F(\lambda x_0^{(1)} + (1 - \lambda)x_0^{(2)}, \lambda u^{(1)} + (1 - \lambda)u^{(2)}) \leq \lambda F(x_0^{(1)}, u^{(1)}) + (1 - \lambda)F(x_0^{(2)}, u^{(2)}).$$

Since  $F(x_0, u)$  is jointly convex in  $(x_0, u)$  and  $\mathcal{U}$  is convex, their partial infimum over  $u \in \mathcal{U}$  preserves convexity (see [Boyd and Vandenberghe \(2004\)](#), p. 87). Under the assumption that  $\eta(\cdot)$  is finite everywhere, we obtain  $\eta(\cdot)$  is a norm.  $\square$

The following result, adapted from Corollary 3.23 of [Brezis \(2011\)](#), ensures the existence of minimizers for coercive convex functions.

**Lemma 2.** *Let  $E$  be a reflexive Banach space and let  $A \subset E$  be a nonempty, closed, convex subset of  $E$ . Let  $\varphi : A \rightarrow (-\infty, +\infty]$  be a convex lower semicontinuous function such that  $\varphi \not\equiv +\infty$  and*

$$\lim_{\substack{x \in A \\ \|x\| \rightarrow \infty}} \varphi(x) = +\infty.$$

*Then  $\varphi$  achieves its minimum on  $A$ , i.e., there exists some  $x_0 \in A$  such that  $\varphi(x_0) = \min_A \varphi$ .*

Following [Hu et al. \(2017\)](#), we introduce the following operator acting on norms.

**Definition 6.** *Given any norm  $\xi$  on  $L^2(\Omega; \mathbb{R}^n)$ , define an operator  $\mathcal{T}$  by*

$$(\mathcal{T}\xi)(x) := \inf_{v \in \mathbb{R}^m} \xi((A + \bar{A}\omega)x + (B + \bar{B}\omega)v), \quad x \in L^2(\Omega; \mathbb{R}^n), \quad (4)$$

*where  $\omega \sim \mathcal{N}(0, \sigma^2)$  is independent of  $(x, v)$ . For brevity, we write  $\xi_{\sharp} := \mathcal{T}\xi$ .*

Unless stated otherwise, all subsequent results are derived under the following nondegeneracy assumption.

**Assumption 1.** *The stacked matrix*

$$U := \begin{bmatrix} B \\ \sigma \bar{B} \end{bmatrix} \in \mathbb{R}^{2n \times m}$$

*has full column rank.*

This condition rules out degenerate input configurations in which the deterministic channel  $B$  and the multiplicative channel  $\bar{B}$  fail to excite some control directions. In particular, for every  $P \succ 0$  it implies

$$B^\top PB + \sigma^2 \bar{B}^\top P \bar{B} \succ 0.$$

Thus, the quadratic forms that appear in the mean-square estimates below are strictly positive. The same assumption will be used again in the constructive part of Section 4. The next theorem provides necessary and sufficient condition ensuring the attainability of  $\rho^*$ .

**Theorem 1.** *The following statements are equivalent.*

$$i) \quad \mathcal{W} = L^2(\Omega; \mathbb{R}^n) \text{ and } \sup_{\|x\|_{\text{ms}}=1} \eta(x) < \infty.$$

ii) There exist an admissible control policy  $u \in \mathcal{U}$  and a constant  $\kappa \geq 0$  such that  $\mathbb{E}[x_k^\top x_k] \leq \kappa(\rho^*)^{2k} \mathbb{E}[x_0^\top x_0]$  holds for all  $k \in \mathbb{N}$ .

*Proof.* (i)  $\Rightarrow$  (ii). We first establish the equivalence between  $\eta(\cdot)$  and the mean-square norm  $\|\cdot\|_{\text{ms}}$ . The lower bound  $\eta(x) \geq \|x\|_{\text{ms}}$  follows directly from  $k = 0$  in (3). For the upper bound, let

$$C := \sup_{\|x\|_{\text{ms}}=1} \eta(x) < \infty.$$

For any  $x \neq 0$ , write  $x = \|x\|_{\text{ms}} \hat{x}$  with  $\|\hat{x}\|_{\text{ms}} = 1$ . Using the positive homogeneity of  $\eta$ , we obtain

$$\eta(x) = \|x\|_{\text{ms}} \eta(\hat{x}) \leq C \|x\|_{\text{ms}}.$$

Thus, together with the lower bound, we have

$$\|x\|_{\text{ms}} \leq \eta(x) \leq C \|x\|_{\text{ms}} \quad (5)$$

for any  $x \in L^2(\Omega; \mathbb{R}^n)$ , showing the equivalence. From the definition in (3), separating the  $k = 0$  term yields

$$\eta(x_0) = \max \left\{ \|x_0\|_{\text{ms}}, \eta_{\sharp}(x_0)/\rho^* \right\},$$

which implies  $\eta_{\sharp}(x) \leq \rho^* \eta(x)$ . Next, for fixed  $x$ , consider

$$f(v) := \eta((A + \bar{A}\omega)x + (B + \bar{B}\omega)v), \quad \omega \sim \mathcal{N}(0, \sigma^2).$$

Since  $\eta$  is equivalent to the mean-square norm  $\|\cdot\|_{\text{ms}}$ , it is a continuous norm on  $L^2(\Omega; \mathbb{R}^n)$ . As  $(A + \bar{A}\omega)x + (B + \bar{B}\omega)v$  is affine in  $v$ , we have that  $f$  is continuous and convex on  $\mathbb{R}^m$ . To check the coercivity, note that  $\eta(\cdot) \geq \|\cdot\|_{\text{ms}}$  gives

$$f(v) \geq \|(B + \bar{B}\omega)v\|_{\text{ms}} - \|(A + \bar{A}\omega)x\|_{\text{ms}}.$$

By the independence of  $\omega$  and  $v$ , we have

$$\|(B + \bar{B}\omega)v\|_{\text{ms}}^2 = \mathbb{E}[v^\top (B + \bar{B}\omega)^\top (B + \bar{B}\omega)v] \geq \lambda_{\min}(B^\top B + \sigma^2 \bar{B}^\top \bar{B}) \|v\|_{\text{ms}}^2,$$

where  $\lambda_{\min}(B^\top B + \sigma^2 \bar{B}^\top \bar{B}) > 0$  by Assumption 1. Hence,

$$f(v) \geq \sqrt{\lambda_{\min}(B^\top B + \sigma^2 \bar{B}^\top \bar{B})} \|v\|_{\text{ms}} - \|(A + \bar{A}\omega)x\|_{\text{ms}}.$$

Thus,  $f$  is coercive, as  $\|v\|_{\text{ms}} \rightarrow \infty$ ,  $f(v) \rightarrow \infty$ . By Lemma 2, the infimum  $\inf_{v \in \mathbb{R}^m} f(v)$  is attained at some  $v^*$ . Therefore,

$$\eta_{\sharp}(x) = \eta((A + \bar{A}\omega)x + (B + \bar{B}\omega)v^*) \leq \rho^* \eta(x).$$

Iterating along the trajectory gives

$$\eta(x_k) \leq (\rho^*)^k \eta(x_0);$$

together with (5), we obtain

$$\|x_k\|_{\text{ms}} \leq \eta(x_k) \leq (\rho^*)^k \eta(x_0) \leq C (\rho^*)^k \|x_0\|_{\text{ms}}.$$

Squaring both sides and letting  $\kappa = C^2$  give (ii).

(ii)  $\Rightarrow$  (i). Assume that there exist an admissible policy  $u$  and  $\kappa \geq 0$  such that

$$\|x_k\|_{\text{ms}} \leq \sqrt{\kappa} (\rho^*)^k \|x_0\|_{\text{ms}}, \quad \forall k \in \mathbb{N}.$$

Then, by the definition of  $\eta$ , it holds

$$\eta(x_0) = \inf_{u \in \mathcal{U}} \sup_{k \geq 0} \frac{\|x_k\|_{\text{ms}}}{(\rho^*)^k} \leq \sup_{k \geq 0} \frac{\|x_k\|_{\text{ms}}}{(\rho^*)^k} \leq \sqrt{\kappa} \|x_0\|_{\text{ms}}.$$

Hence, we know  $\eta(x) < \infty$  for all  $x$ ,  $\mathcal{W} = L^2(\Omega; \mathbb{R}^n)$ , and  $\sup_{\|x\|_{\text{ms}}=1} \eta(x) \leq \sqrt{\kappa} < \infty$ . Thus, (i) holds.  $\square$

While the necessary and sufficient condition ensuring *exact attainability* of  $\rho^*$  is theoretically sound, it is also rather restrictive and may be difficult to be verified in practice. Nevertheless, one can still derive meaningful and verifiable *sufficient conditions* that yield computable *upper and lower bounds* for  $\rho^*$ . Following the norm-based methodology of [Hu et al. \(2017\)](#), we now extend these bounding arguments to the stochastic setting considered here.

**Proposition 2.** *Let  $\xi(\cdot) = \|\cdot\|_{\text{ms}}$ . Then, the following assertions hold.*

- i) *If  $\xi_{\sharp}(\cdot) \geq \alpha \xi(\cdot)$  for some  $\alpha \geq 0$ , then  $\rho^* \geq \alpha$ ;*
- ii) *If  $\xi_{\sharp}(\cdot) \leq \beta \xi(\cdot)$  for some  $\beta \geq 0$ , then  $\rho^* \leq \beta$ .*

*Proof.* The proof of part (i) is similar to that of [Hu et al. \(2017\)](#) and is omitted here. For part (ii), we first establish the existence of a minimizer. Fix  $x_k$  and consider the one-step optimization problem

$$\begin{aligned} & \inf_{v \in \mathbb{R}^m} \xi^2((A + \bar{A}\omega)x + (B + \bar{B}\omega)v) \\ &= \inf_{v \in \mathbb{R}^m} \mathbb{E}\{x^{\top}(A^{\top}A + \sigma^2\bar{A}^{\top}\bar{A})x + 2x^{\top}(A^{\top}B + \sigma^2\bar{A}^{\top}\bar{B})v + v^{\top}(B^{\top}B + \sigma^2\bar{B}^{\top}\bar{B})v\}; \end{aligned}$$

the minimizer  $v^* = (B^{\top}B + \sigma^2\bar{B}^{\top}\bar{B})^{-1}(B^{\top}A + \sigma^2\bar{B}^{\top}\bar{A})x$  exists. With this choice of  $v^*$ , we obtain

$$\xi(x_{k+1}) = \|(A + \bar{A}\omega_k)x_k + (B + \bar{B}\omega_k)v_k^*\|_{\text{ms}} = \xi_{\sharp}(x_k) \leq \beta \xi(x_k). \quad (6)$$

Iterating (6) yields

$$\xi(x_k) \leq \beta^k \xi(x_0).$$

Hence,  $\rho^* \leq \beta$ . □

This completes the extension of the norm-based framework of [Hu et al. \(2017\)](#) to our stochastic setting. In the next section, we develop an alternative viewpoint based on an optimal control reformulation.

## 4 Optimal Control Reformulation of Problem (OSR)

In this section, we reformulate Problem (OSR) of computing the optimal stabilizing rate as an optimal control problem. The first step is to introduce a cost functional that quantifies the exponential mean-square growth rate of system state. For an initial state  $x_0 \neq 0$  and control policy  $u \in \mathcal{U}$ , define

$$J(x_0, u) := \limsup_{k \rightarrow \infty} \frac{1}{k} \log \left( \frac{\mathbb{E}[x_k^{\top} x_k]}{\mathbb{E}[x_0^{\top} x_0]} \right).$$

This functional represents the asymptotic logarithmic rate of growth of the expected state energy. When  $J(x_0, u) < 0$ , the state will converge exponentially to the origin in the mean-square sense.

The following theorem establishes the precise relationship between the cost  $J(x_0, u)$  and the stabilizing rate  $\rho(u)$ , demonstrating that both provide equivalent quantitative characterizations of mean-square exponential stability.

**Theorem 3.** *For each admissible control policy  $u \in \mathcal{U}$ , the functionals  $J(x_0, u)$  and  $\rho(u)$  satisfy*

$$J(x_0, u) = 2 \log \rho(u).$$

Consequently, it holds

$$\inf_{u \in \mathcal{U}} J(x_0, u) = 2 \log \left( \inf_{u \in \mathcal{U}} \rho(u) \right).$$

Moreover, if either  $\inf_{u \in \mathcal{U}} J(x_0, u)$  or  $\inf_{u \in \mathcal{U}} \rho(u)$  is attained by some admissible policy, then so is the other, and their minimizers coincide

$$\arg \min_{u \in \mathcal{U}} J(x_0, u) = \arg \min_{u \in \mathcal{U}} \rho(u).$$

*Proof.* For any  $u \in \mathcal{U}$ , by the definition of  $\rho(u)$  and for any  $\varepsilon_1 > 0$ , there exists  $\tilde{\kappa} \geq 0$  such that

$$\mathbb{E}[x_k^\top x_k] \leq \tilde{\kappa}(\rho(u) + \varepsilon_1)^{2k} \mathbb{E}[x_0^\top x_0], \quad \forall k \in \mathbb{N}.$$

Hence, it holds

$$J(x_0, u) = \limsup_{k \rightarrow \infty} \frac{1}{k} \log \left( \frac{\mathbb{E}[x_k^\top x_k]}{\mathbb{E}[x_0^\top x_0]} \right) \leq 2 \log(\rho(u) + \varepsilon_1).$$

Since  $\varepsilon_1 > 0$  is arbitrary, this gives

$$J(x_0, u) \leq 2 \log \rho(u). \quad (7)$$

Conversely, let  $J(x_0, u) = \alpha$ , then for any  $\varepsilon_2 > 0$  there exists  $N$  such that for all  $k > N$  it holds

$$\mathbb{E}[x_k^\top x_k] \leq \mathbb{E}[x_0^\top x_0] e^{k(\alpha+\varepsilon_2)} = \mathbb{E}[x_0^\top x_0] (e^{(\alpha+\varepsilon_2)/2})^{2k}.$$

Let  $\rho_1 := e^{(\alpha+\varepsilon_2)/2}$  and choose

$$\kappa := \max \left\{ 1, \max_{0 \leq k \leq N} \frac{\mathbb{E}[x_k^\top x_k]}{\mathbb{E}[x_0^\top x_0] \rho_1^{2k}} \right\} < \infty.$$

Then,  $\mathbb{E}[x_k^\top x_k] \leq \kappa \rho_1^{2k} \mathbb{E}[x_0^\top x_0]$  holds for all  $k \in \mathbb{N}$ , and by the definition of  $\rho(u)$ , we have  $\rho(u) \leq \rho_1$ . Since  $\varepsilon_2 > 0$  is arbitrary, we get  $\rho(u) \leq e^{\alpha/2}$ , i.e.,

$$\rho(u) \leq e^{J(x_0, u)/2} \Rightarrow 2 \log \rho(u) \leq J(x_0, u). \quad (8)$$

Since (7) and (8) hold in the opposite directions for each admissible control  $u \in \mathcal{U}$ , we obtain the equality

$$J(x_0, u) = 2 \log \rho(u).$$

Taking the infimum over  $u$  on both sides and using the monotonicity of function  $\log$  on  $(0, \infty)$ , we establish

$$\inf_{u \in \mathcal{U}} J(x_0, u) = 2 \log \left( \inf_{u \in \mathcal{U}} \rho(u) \right).$$

Finally, if  $u^*$  minimizes  $J(x_0, u)$ , then  $\rho(u^*) \leq e^{\inf J(x_0, u)/2} = \inf \rho$ , therefore  $u^*$  also minimizes  $\rho$ ; the converse direction is similar, giving  $\arg \min J = \arg \min \rho$ .  $\square$

In the sequel, we will analyze the stabilization problem in a statewise manner. For this purpose, it is convenient to restrict the admissible controls to policies that depend only on the current state. Accordingly, we introduce the admissible feedback policies

$$\mathcal{U}_{\text{fb}} := \left\{ u = (u_0, u_1, \dots) \mid u_k = \mu_k(x_k), \mu_k : \mathbb{R}^n \rightarrow \mathbb{R}^m, \mathbb{E}[u_k^\top u_k] < \infty \right\},$$

where  $\{x_k\}$  denotes the state trajectory of system (1) driven by  $u$ , and  $\mathcal{U}_{\text{fb}}$  is a subclass of the original admissible set  $\mathcal{U}$ . We emphasize that this restriction is imposed for technical reasons: working with feedback policies allows us to express all state trajectories in terms of a state-dependent performance function, which will be needed for the subsequent analysis. It is not claimed that feedback policies exhaust all admissible stabilizing policies; nevertheless, [Ni et al. \(2015\)](#) shows that for linear stochastic systems, open-loop  $\ell^2$ -stabilizable is equivalent to closed-loop  $\ell^2$ -stabilizable. Our use of feedback policies is therefore a structural restriction that facilitates the development of our framework, without making any claim about optimality of feedback relative to the general class  $\mathcal{U}$ . In particular, since  $\mathcal{U}_{\text{fb}} \subseteq \mathcal{U}$ , the identity of Theorem 3 continues to hold when the admissible set is restricted to  $\mathcal{U}_{\text{fb}}$ ; namely,

$$\inf_{u \in \mathcal{U}_{\text{fb}}} J(x_0, u) = 2 \log \left( \inf_{u \in \mathcal{U}_{\text{fb}}} \rho(u) \right).$$

Having established the general relationship between  $J(x_0, u)$  and  $\rho(u)$ , we now formulate the corresponding optimal control problem.

**Problem (OC).** Solve the optimization problem

$$\begin{aligned} \inf_{u \in \mathcal{U}_{\text{fb}}} \quad & J(x_0, u) = \limsup_{k \rightarrow \infty} \frac{1}{k} \log \left( \frac{\mathbb{E}[x_k^\top x_k]}{\mathbb{E}[x_0^\top x_0]} \right), \\ \text{s.t.} \quad & x_{k+1} = (A + \bar{A}\omega_k)x_k + (B + \bar{B}\omega_k)u_k, \quad k \in \mathbb{N}. \end{aligned} \quad (9)$$

**Theorem 4.** Suppose there exist a scalar  $\lambda \in \mathbb{R}$  and a quadratic function  $h(x) = x^\top Px$  with  $P \in \mathbb{S}_{++}^n$  such that for every  $x \in \mathbb{R}^n$ ,

$$e^\lambda h(x) = \inf_{\mu: \mathbb{R}^n \rightarrow \mathbb{R}^m} \mathbb{E}[h((A + \bar{A}\omega)x + (B + \bar{B}\omega)\mu(x)) | x], \quad \omega \sim \mathcal{N}(0, \sigma^2) \quad (10)$$

holds. Then, for any state feedback control policy  $u \in \mathcal{U}_{\text{fb}}$ , the associated cost functional satisfies

$$J(x_0, u) \geq \lambda.$$

Moreover, if there exists a feedback law  $\mu^* : \mathbb{R}^n \rightarrow \mathbb{R}^m$  attaining the infimum in (10) for all  $x$ , and let  $u_k^* = \mu^*(x_k)$  for all  $k$ , then  $u^* = (u_0^*, u_1^*, \dots)$  is optimal within  $\mathcal{U}_{\text{fb}}$  and

$$J(x_0, u^*) = \lambda.$$

*Proof.* Fix an arbitrary admissible feedback policy  $u = (u_0, u_1, \dots) \in \mathcal{U}_{\text{fb}}$ , and let  $\{x_k\}$  be the state process generated by (1). For each time  $k$ , applying (10) at the current state  $x_k$  gives

$$\begin{aligned} e^\lambda h(x_k) &= \inf_{\mu: \mathbb{R}^n \rightarrow \mathbb{R}^m} \mathbb{E}[h((A + \bar{A}\omega_k)x_k + (B + \bar{B}\omega_k)\mu(x_k)) | x_k] \\ &\leq \mathbb{E}[h((A + \bar{A}\omega_k)x_k + (B + \bar{B}\omega_k)u_k) | x_k]. \end{aligned}$$

Taking expectations and iterating this inequality over  $k$  yield

$$\mathbb{E}[h(x_k) | x_0] \geq e^{k\lambda} h(x_0), \quad k \in \mathbb{N}. \quad (11)$$

Since  $P \succ 0$ , its eigenvalues satisfy

$$\lambda_{\min}(P) \mathbb{E}[x_k^\top x_k] \leq \mathbb{E}[h(x_k)] \leq \lambda_{\max}(P) \mathbb{E}[x_k^\top x_k],$$

and the same bounds hold for  $x_0$ . Combining these relations gives

$$\lambda \leq \frac{1}{k} \log \left( \frac{\mathbb{E}[x_k^\top x_k]}{\mathbb{E}[x_0^\top x_0]} \right) + \frac{1}{k} \log \left( \frac{\lambda_{\max}(P)}{\lambda_{\min}(P)} \right). \quad (12)$$

Applying  $\limsup$  to (12) yields

$$J(x_0, u) \geq \lambda.$$

Now, suppose there exists a feedback law  $\mu^*$  attaining the infimum in (10) for every  $x$ . Define the corresponding stationary feedback policy by  $u_k^* = \mu^*(x_k)$  for all  $k$ . Then, equality holds in the above (11), and thus

$$\mathbb{E}[h(x_k^*) | x_0] = e^{k\lambda} h(x_0), \quad k \in \mathbb{N},$$

where  $\{x_k^*\}$  is the state trajectory under control policy  $u^*$ . Using again the eigenvalue bounds of  $P$  gives

$$\begin{aligned} \frac{1}{k} \log \left( \frac{\lambda_{\min}(P)}{\lambda_{\max}(P)} \right) + \frac{1}{k} \log \left( \frac{\mathbb{E}[(x_k^*)^\top x_k]}{\mathbb{E}[(x_0^*)^\top x_0]} \right) &\leq \frac{1}{k} \log \left( \frac{\mathbb{E}[h(x_k^*)]}{\mathbb{E}[h(x_0)]} \right) = \lambda \\ &\leq \frac{1}{k} \log \left( \frac{\lambda_{\max}(P)}{\lambda_{\min}(P)} \right) + \frac{1}{k} \log \left( \frac{\mathbb{E}[(x_k^*)^\top x_k]}{\mathbb{E}[(x_0^*)^\top x_0]} \right) \end{aligned}$$

Applying  $\limsup$  to above inequality yields

$$J(x_0, u^*) = \limsup_{k \rightarrow \infty} \frac{1}{k} \log \left( \frac{\mathbb{E}[(x_k^*)^\top x_k^*]}{\mathbb{E}[x_0^\top x_0]} \right) = \lambda.$$

Since we have already proved  $J(x_0, u) \geq \lambda$  for all  $u \in \mathcal{U}_{\text{fb}}$ ,  $\mu^*$  is optimal among feedback policies.  $\square$

**Remark.** Equation (10) is not the exact Bellman equation associated with Problem (OC), since the logarithmic growth rate in  $J$  does not admit a direct additive decomposition. Nevertheless, it serves as a powerful surrogate: if a positive-definite quadratic solution exists, it provides a rigorous lower bound on  $J(x_0, u)$  and coincides with the optimal value when the infimum is attained. Hence, we shall refer to (10) as a Bellman-type equation in the remainder of the paper.

For any  $P \in \mathbb{S}_{++}^n$ , define the standard Riccati-type blocks

$$R(P) := B^\top PB + \sigma^2 \bar{B}^\top P \bar{B}, \quad S(P) := A^\top PB + \sigma^2 \bar{A}^\top P \bar{B},$$

and the associated operator

$$\Phi(P) := A^\top PA + \sigma^2 \bar{A}^\top P \bar{A} - S(P) R(P)^{-1} S(P)^\top, \quad (13)$$

together with the feedback gain

$$K(P) := R(P)^{-1} S(P)^\top. \quad (14)$$

Under Assumption 1,  $R(P) \succ 0$ , ensuring that the inverse in (13) is well-defined. If  $P$  is only positive semi-definite,  $R(P)$  may fail to be invertible; in this case, the operator  $\Phi(P)$  is defined by replacing the inverse with the Moore-Penrose generalized inverse:

$$\Phi(P) := A^\top PA + \sigma^2 \bar{A}^\top P \bar{A} - S(P) R(P)^\dagger S(P)^\top,$$

where  $R(P)^\dagger$  denotes the Moore-Penrose generalized inverse (Penrose (1955)).

**Proposition 5.** *The following statements are equivalent.*

- i) There exists  $(\lambda, h(\cdot))$  with  $h(x) = x^\top Px$ ,  $P \in \mathbb{S}_{++}^n$ , satisfying the Bellman-type equation (10).
- ii) There exists  $(\gamma, P) \in \mathbb{R}_+ \times \mathbb{S}_{++}^n$  such that

$$\Phi(P) = \gamma P, \quad \gamma = e^\lambda. \quad (15)$$

Equation (15) thus represents a nonlinear matrix eigenvalue problem.

In this case, the feedback policy achieving the infimum in (10) is  $\mu^*(x) = -K(P)x$  with  $K(P)$  defined in (14).

*Proof.* Suppose (i) holds. For any state  $x \in \mathbb{R}^n$ , consider a control law  $\mu(\cdot)$  applied at this state. Substituting  $h(x)$  into (10) then gives the quadratic optimization problem

$$\begin{aligned} & \inf_{\mu: \mathbb{R}^n \rightarrow \mathbb{R}^m} \mathbb{E} \left[ h((A + \bar{A}\omega)x + (B + \bar{B}\omega)\mu(x)) \mid x \right] \\ &= \inf_{\mu: \mathbb{R}^n \rightarrow \mathbb{R}^m} \left\{ x^\top (A^\top PA + \sigma^2 \bar{A}^\top P \bar{A})x + 2x^\top (A^\top PB + \sigma^2 \bar{A}^\top P \bar{B})\mu(x) \right. \\ & \quad \left. + (\mu(x))^\top (B^\top PB + \sigma^2 \bar{B}^\top P \bar{B})\mu(x) \right\}, \end{aligned} \quad (16)$$

where  $\omega \sim \mathcal{N}(0, \sigma^2)$  is independent of  $x$ . By Assumption 1,  $B^\top PB + \sigma^2 \bar{B}^\top P \bar{B} \succ 0$  and thus the problem has unique minimizer

$$\mu^*(x) = -K(P)x.$$

Therefore, the Bellman-type equation (10) reduces exactly to the nonlinear eigenvalue problem  $\Phi(P) = \gamma P$ .

Conversely, suppose there exist  $P \succ 0$  and  $\gamma > 0$  such that  $\Phi(P) = \gamma P$ . Then, for  $h(x) = x^\top P x$  and control  $\mu^*(x) = -K(P)x$ , we obtain

$$\inf_{\mu: \mathbb{R}^n \rightarrow \mathbb{R}^m} \mathbb{E}[h((A + \bar{A}\omega)x + (B + \bar{B}\omega)\mu(x))|x] = x^\top \Phi(P)x = \gamma h(x);$$

this shows that  $\Phi(P) \succeq 0$  and  $(\lambda, h)$  with  $\lambda = \log \gamma$  solves the Bellman-type equation (10). This proves the equivalence.  $\square$

This equivalence reduces the search for solutions of (10) to a nonlinear matrix eigenvalue problem of the form  $\Phi(P) = \gamma P$ . In the next section, we establish the existence of strictly positive-definite fixed points for a perturbed version of equation (15) by introducing a regularization scheme, which also leads to computable performance bounds for  $\rho^*$ .

## 5 Regularized Approximations and Certified Performance Bounds

In this section, we develop a constructive framework for analyzing and computing solutions of the nonlinear eigenvalue matrix equation (15). The framework addresses both the existence of strictly positive-definite solutions and the computation of certified performance bounds. It is organized around three mutually reinforcing components.

- i) **Regularized Existence Guarantee.** Direct attempts to solve (15) may lead only to semi-definite solutions. To ensure strictly positive definite fixed points, we introduce a regularization parameter  $\tau \in (0, 1)$  and construct a regularized normalized operator  $\hat{\Phi}_\tau$  defined in (20). The corresponding fixed points  $P^{(\tau)} \succ 0$  is well-defined and serve as approximation to the true solution of (15).
- ii) **Certified Performance Bounds.** The fixed point  $P^{(\tau)}$  provides computable information on the optimal cost  $J^*$  and optimal stabilizing rate  $\rho^*$ . Quadratic test functions yield explicit lower bounds, while the feedback policy induced by  $P^{(\tau)}$  provides computable upper bounds. Together, these results provide computable bounds for  $J^*$  and  $\rho^*$ .
- iii) **Regularized Value Iteration Algorithm.** To compute  $P^{(\tau)}$  in practice, we propose a *regularized normalized value iteration* (RNVI) algorithm. For sufficiently large  $\tau$ , we establish global contraction via explicit Lipschitz constants, and then employ a continuation strategy to extend the convergence guarantees to smaller  $\tau$ .

Taken together, these elements yield a unified algorithm that produces both the regularized approximations  $P^{(\tau)}$  and the certified performance bounds for the optimal stabilizing rate. For clarity, we summarize the constants and notations used throughout this section. Define

$$R_0 := B^\top B + \sigma^2 \bar{B}^\top \bar{B}, \quad C_A := \lambda_{\max}(AA^\top + \sigma^2 \bar{A}\bar{A}^\top). \quad (17)$$

For a regularization parameter  $\tau \in (0, 1)$ , set

$$\delta_\tau := \frac{\frac{\tau}{n}}{(1 - \tau)C_A + \tau}. \quad (18)$$

We further denote the following auxiliary constants that appear in the Lipschitz analysis:

$$\alpha_A := \|A\|^2 + \sigma^2 \|\bar{A}\|^2, \quad \alpha_S := \|A\| \|B\| + \sigma^2 \|\bar{A}\| \|\bar{B}\|, \quad \alpha_R := \|B\|^2 + \sigma^2 \|\bar{B}\|^2. \quad (19)$$

## 5.1 Existence of Regularized Positive-Definite Solutions

The nonlinear matrix eigenvalue equation (15) may in general admit only semi-definite solutions. To ensure strictly positive-definite fixed points, we introduce a *regularized normalization scheme*, which forms the foundation of our subsequent fixed-point analysis.

**Definition 7.** For  $\tau \in (0, 1)$ , define

$$\widehat{\Phi}_\tau(P) := \frac{(1 - \tau)\Phi(P) + \frac{\tau}{n}I}{\text{Tr}((1 - \tau)\Phi(P) + \frac{\tau}{n}I)}, \quad P \in \mathbb{S}_{++}^n. \quad (20)$$

This operator interpolates between the unregularized map  $\frac{\Phi}{\text{Tr}\Phi}$  (as  $\tau \rightarrow 0$ ) and the uniform normalization  $I/n$  (as  $\tau \rightarrow 1$ ), ensuring that its image always remains in the interior of the cone  $\mathbb{S}_+^n$ . We recall Brouwers fixed-point theorem, which provides the existence of fixed points for continuous self-maps on compact convex sets (see, e.g., Theorem 8.1.3 of [Borwein and Lewis \(2006\)](#)). A self map refers to a mapping whose domain and range coincide.

**Theorem 6** (Brouwer). *Any continuous self map of a nonempty compact convex subset of a finite-dimensional Euclidean space has a fixed point.*

**Theorem 7.** For each  $\tau \in (0, 1)$ , there exists  $P^{(\tau)} \succ 0$  with  $\text{Tr} P^{(\tau)} = 1$  such that

$$\widehat{\Phi}_\tau(P^{(\tau)}) = P^{(\tau)}, \quad (21)$$

where  $\widehat{\Phi}_\tau(\cdot)$  is defined in (20).

*Proof.* For any  $P \succeq 0$  with  $\text{Tr} P = 1$ , note that

$$\text{Tr} \Phi(P) \leq \text{Tr}(P(AA^\top + \sigma^2 \bar{A}\bar{A}^\top)) \leq C_A$$

with  $C_A$  defined in (17). Hence, for any  $\tau \in (0, 1)$ , it holds

$$(1 - \tau)\Phi(P) + \frac{\tau}{n}I \succeq \frac{\tau}{n}I, \quad \text{Tr}((1 - \tau)\Phi(P) + \frac{\tau}{n}I) \leq (1 - \tau)C_A + \tau.$$

Then, the regularized operator  $\widehat{\Phi}_\tau(P)$  satisfies

$$\lambda_{\min}(\widehat{\Phi}_\tau(P)) = \frac{\lambda_{\min}((1 - \tau)\Phi(P) + \frac{\tau}{n}I)}{\text{Tr}((1 - \tau)\Phi(P) + \frac{\tau}{n}I)} \geq \frac{\frac{\tau}{n}}{(1 - \tau)C_A + \tau} = \delta_\tau > 0.$$

Define the trace-normalized slice

$$\mathcal{S}_{\delta_\tau} := \left\{ X \in \mathbb{S}_{++}^n : X \succeq \delta_\tau I, \text{Tr}(X) = 1 \right\}.$$

Since  $\delta_\tau \leq 1/n$ , we have  $I/n \in \mathcal{S}_{\delta_\tau}$ , which shows that the set  $\mathcal{S}_{\delta_\tau}$  is nonempty; moreover, this set is convex and compact. By its construction,  $\widehat{\Phi}_\tau : \mathcal{S}_{\delta_\tau} \rightarrow \mathcal{S}_{\delta_\tau}$  is a continuous mapping. Thus, by Theorem 6, there exists  $P^{(\tau)} \in \mathcal{S}_{\delta_\tau}$  with  $\widehat{\Phi}_\tau(P^{(\tau)}) = P^{(\tau)}$ .  $\square$

Having established the existence of strictly positive definite fixed points for each  $\tau > 0$ , we now investigate the behavior as the regularization parameter tends to zero.

**Theorem 8.** Let  $\{\tau_j\}_{j \geq 1}$  be a decreasing sequence in  $(0, 1)$  with  $\tau_j \downarrow 0$ . For each  $\tau_j$ , let  $P^{(\tau_j)}$  be the regularized fixed point from Theorem 7, and define

$$\gamma^{(\tau_j)} := \text{Tr}((1 - \tau_j)\Phi(P^{(\tau_j)}) + \frac{\tau_j}{n}I).$$

Then, there exist a subsequence (not relabelled), and limits  $P^* \succeq 0$  and  $\gamma^* \in [0, C_A]$ , such that

$$P^{(\tau_j)} \rightarrow P^*, \quad \gamma^{(\tau_j)} \rightarrow \gamma^*, \quad \Phi(P^{(\tau_j)}) \rightarrow \gamma^* P^*$$

as  $j \rightarrow \infty$ .

*Proof.* By Theorem 7 and for any  $\tau \in (0, 1)$ , the regularized fixed point  $P^{(\tau)}$  satisfies  $P^{(\tau)} \succeq 0$  and  $\text{Tr } P^{(\tau)} = 1$ . Hence, for each  $j$ , it holds

$$P^{(\tau_j)} \in S := \{X \succeq 0 : \text{Tr } X = 1\}.$$

The set  $S$  is compact and thus the sequence  $\{P^{(\tau_j)}\}$  admits a convergent subsequence. Passing to this subsequence and not relabelling, we obtain

$$P^{(\tau_j)} \rightarrow P^* \quad \text{for some } P^* \succeq 0 \text{ when } j \rightarrow \infty.$$

Next, by Theorem 7, we also have

$$\gamma^{(\tau_j)} \rightarrow \gamma^* \quad \text{for some } \gamma^* \in [0, C_A] \text{ when } j \rightarrow \infty.$$

For each  $j$ , the fixed point relation from Theorem 7 yields

$$P^{(\tau_j)} = \frac{(1 - \tau_j) \Phi(P^{(\tau_j)}) + \frac{\tau_j}{n} I}{\text{Tr}((1 - \tau_j) \Phi(P^{(\tau_j)}) + \frac{\tau_j}{n} I)} = \frac{(1 - \tau_j) \Phi(P^{(\tau_j)}) + \frac{\tau_j}{n} I}{\gamma^{(\tau_j)}}.$$

Rearranging above equation gives

$$\Phi(P^{(\tau_j)}) = \frac{\gamma^{(\tau_j)} P^{(\tau_j)} - \frac{\tau_j}{n} I}{1 - \tau_j}.$$

Since  $P^{(\tau_j)} \rightarrow P^*$ ,  $\gamma^{(\tau_j)} \rightarrow \gamma^*$  as  $j \rightarrow \infty$ , we have

$$\gamma^{(\tau_j)} P^{(\tau_j)} - \frac{\tau_j}{n} I \rightarrow \gamma^* P^*, \quad 1 - \tau_j \rightarrow 1,$$

and therefore,

$$\Phi(P^{(\tau_j)}) \rightarrow \gamma^* P^*$$

holds. This proves the claim.  $\square$

**Remark.** The limiting matrix  $P^*$  may in general lie on the boundary of  $\mathbb{S}_+^n$ , and thus fail to be strictly positive definite. Nevertheless, the regularization procedure ensures that for every  $\tau > 0$  the approximation  $P^{(\tau)}$  remains strictly positive definite, thereby providing a family of well-conditioned surrogates approaching  $P^*$ . As shown in the next subsection, these approximations also enable the derivation of explicit lower and upper bounds for the optimal stabilizing rate  $\rho^*$ , thus yielding computable near-optimality guarantees.

## 5.2 Certified Performance Bounds

In this subsection, we leverage the regularized fixed points established in Theorem 7 to derive the certified performance guarantees. Quadratic test functions yield universal lower bounds for the optimal stabilizing rate, while the feedback policies induced by the regularized fixed points provide computable upper bounds. Together, these results lead to two-sided estimates for the optimal stabilizing rate  $\rho^*$ .

**Lemma 3.** Let  $P \in \mathbb{S}_{++}^n$  and define

$$L(P) := \lambda_{\min}(P^{-1/2} \Phi(P) P^{-1/2}), \quad U(P) := \lambda_{\max}(P^{-1/2} \Phi(P) P^{-1/2}),$$

where  $\Phi(P)$  is given by (13). Then, for all  $x \in \mathbb{R}^n$ , it holds

$$L(P) h_P(x) \leq x^\top \Phi(P) x \leq U(P) h_P(x)$$

with  $h_P(x) = x^\top P x$ .

*Proof.* Set  $y := P^{1/2}x$ . Then, we obtain

$$x^\top \Phi(P)x = y^\top (P^{-1/2}\Phi(P)P^{-1/2})y, \quad h_P(x) = y^\top y.$$

The bounds follow immediately from the min-max characterization of eigenvalues.  $\square$

The next result shows that every quadratic test function yields a lower bound for cost  $J$  and the bound is nontrivial whenever  $L(P) > 0$ .

**Proposition 9.** *For  $P \in \mathbb{S}_{++}^n$ , let  $L(P)$  be given in Lemma 3. For any admissible policy  $u \in \mathcal{U}_{\text{fb}}$ , it holds*

$$J(x_0, u) \geq \log L(P).$$

In particular,

$$J^* = \inf_{u \in \mathcal{U}_{\text{fb}}} J(x_0, u) \geq \sup_{P \succ 0} \log L(P).$$

*Proof.* For each  $x_k$ , applying (10) to  $x_k$  yields

$$\min_{u_k} \mathbb{E}[h_P(x_{k+1}) \mid x_k] = x_k^\top \Phi(P) x_k \geq L(P) h_P(x_k),$$

where the inequality follows from Lemma 3. Hence, under any policy  $u \in \mathcal{U}_{\text{fb}}$ , taking expectations and iterating above inequality yield

$$\mathbb{E}[h_P(x_k)] \geq (L(P))^k \mathbb{E}[h_P(x_0)].$$

Since  $P \succ 0$ , we have

$$\lambda_{\min}(P) \mathbb{E}[x_k^\top x_k] \leq \mathbb{E}[h_P(x_k)] \leq \lambda_{\max}(P) \mathbb{E}[x_k^\top x_k].$$

The exponential growth rates of  $\mathbb{E}[h_P(x_k)]$  and  $\mathbb{E}[x_k^\top x_k]$  coincide. Thus,  $J(x_0, u) \geq \log L(P)$ , and taking the infimum over  $u$  establishes the claim.  $\square$

**Remark.** Proposition 9 holds for every  $P \succ 0$ , implying

$$J^* \geq \sup_{P \succ 0} \log L(P).$$

The term  $\sup_{P \succ 0} L(P)$  depends only on the system matrices and represents the sharpest lower bound achievable by quadratic test functions. If a strictly positive-definite eigen-solution  $P$  of  $\Phi(P) = \gamma P$  exists, this inequality becomes an equality. In practice, however, directly maximizing  $L(P)$  is computationally intractable. Instead, one evaluates  $L(P)$  at the regularized fixed points  $P^{(\tau)}$  defined in (21), which are computable via the regularized operator  $\hat{\Phi}_\tau$ .

We now turn to upper bounds for the optimal cost  $J^*$ . For each  $\tau \in (0, 1)$ , recall from Definition 7 and Theorem 7 that  $\hat{\Phi}_\tau(P^{(\tau)}) = P^{(\tau)}$  admits a strictly positive-definite solution with trace one. Let

$$\mu_{(\tau)}^*(x) := -K(P^{(\tau)})x \tag{22}$$

denote the corresponding optimal feedback law that solves the Bellman-type equation (10) with  $h(x) = x^\top P^{(\tau)}x$ . Since  $P^{(\tau)}$  approximates the unregularized fixed point as  $\tau \downarrow 0$ , the gain  $K(P^{(\tau)})$  may be viewed as a near-optimal gain.

**Proposition 10.** *For  $\tau \in (0, 1)$ , let  $P^{(\tau)} \succ 0$  solve equation (21) and define*

$$\gamma^{(\tau)} := \text{Tr}\left((1 - \tau)\Phi(P^{(\tau)}) + \frac{\tau}{n}I\right).$$

*Then, the cost functional  $J(x_0, \cdot)$  under feedback control  $u_{(\tau)}^* = (\mu_{(\tau)}^*(x_0), \dots)$  defined in (22) satisfies*

$$\inf_{u \in \mathcal{U}_{\text{fb}}} J(x_0, u) \leq J(x_0, u_{(\tau)}^*) \leq \log\left(\frac{\gamma^{(\tau)}}{1 - \tau}\right).$$

*Proof.* From (21), for any  $x$ , it holds

$$(1 - \tau) x^\top \Phi(P^{(\tau)}) x + \frac{\tau}{n} x^\top x = \gamma^{(\tau)} h_{P^{(\tau)}}(x) \quad \text{with } h_{P^{(\tau)}}(x) = x^\top P^{(\tau)} x.$$

Then, rearranging above equation gives

$$x^\top \Phi(P^{(\tau)}) x = \frac{\gamma^{(\tau)} h_{P^{(\tau)}}(x) - \frac{\tau}{n} x^\top x}{1 - \tau} \leq \frac{\gamma^{(\tau)}}{1 - \tau} h_{P^{(\tau)}}(x).$$

Under  $u_{(\tau)}^*$ , we have

$$\mathbb{E}[h_{P^{(\tau)}}(x_{k+1}) \mid x_k] = x_k^\top \Phi(P^{(\tau)}) x_k \leq \frac{\gamma^{(\tau)}}{1 - \tau} \mathbb{E}[h_{P^{(\tau)}}(x_k)].$$

Iterating above inequality over  $k$  shows that  $\mathbb{E}[h_{P^{(\tau)}}(x_k)]$  grows at most at rate  $(\gamma^{(\tau)} / (1 - \tau))^k$ ; this yields the stated upper bound on  $J(x_0, u_{(\tau)}^*)$ .  $\square$

The following result summarizes the main result of this paper, providing explicit two-sided bounds that certify the optimal stabilizing rate.

**Theorem 11.** *For any  $\tau \in (0, 1)$  and any solution  $P^{(\tau)} \succ 0$  of (21), the optimal cost satisfies*

$$\log L(P^{(\tau)}) \leq J^* \leq \log\left(\frac{\gamma^{(\tau)}}{1 - \tau}\right), \quad (23)$$

where  $L(P^{(\tau)})$  is defined in Lemma 3 and  $\gamma^{(\tau)}$  is in Proposition 10. Equivalently, recalling from Theorem 3 that  $J^* = 2 \log \rho^*$ , it holds

$$\sqrt{L(P^{(\tau)})} \leq \rho^* \leq \sqrt{\frac{\gamma^{(\tau)}}{1 - \tau}}.$$

Having obtained computable upper and lower bounds for  $\rho^*$  in Theorem 11, we next analyze how tight these bounds are as  $\tau$  varies.

**Theorem 12.** *For any  $\tau \in (0, 1)$  and any solution  $P^{(\tau)}$  of (21), define*

$$L_\tau := L(P^{(\tau)}), \quad U_\tau := \frac{\gamma^{(\tau)}}{1 - \tau}, \quad \Delta_\tau := U_\tau - L_\tau.$$

Then, the following statements hold.

(i) *The gap between the squared certified bounds for  $\rho^*$  in Theorem 11 admits the explicit expression*

$$\Delta_\tau = \frac{\tau}{n(1 - \tau)} \lambda_{\max}((P^{(\tau)})^{-1}).$$

(ii) *Let  $\{\tau_k\}_{k \geq 1} \subset (0, 1)$  with  $\tau_k \downarrow 0$ , and let  $P^* \succeq 0$  be a limit point of  $\{P^{(\tau_k)}\}$  as characterized in Theorem 8. If the limit satisfies  $P^* \succ 0$ , then the certified squared bound becomes asymptotically tight along the corresponding convergent subsequence:*

$$\Delta_{\tau_k} \rightarrow 0 \quad \text{as } k \rightarrow \infty.$$

*Proof.* Fix  $\tau \in (0, 1)$  and a corresponding fixed point  $P^{(\tau)} \succ 0$  of (21). By the fixed-point relation (21), it holds

$$(1 - \tau) \Phi(P^{(\tau)}) + \frac{\tau}{n} I = \gamma^{(\tau)} P^{(\tau)}.$$

Multiplying by  $(P^{(\tau)})^{-1/2}$  on both sides of above equation and rearranging it yields

$$(1 - \tau) (P^{(\tau)})^{-1/2} \Phi(P^{(\tau)}) (P^{(\tau)})^{-1/2} = \gamma^{(\tau)} I - \frac{\tau}{n} (P^{(\tau)})^{-1}.$$

Hence, the eigenvalues of  $(P^{(\tau)})^{-1/2}\Phi(P^{(\tau)})(P^{(\tau)})^{-1/2}$  are

$$\lambda_i = \frac{\gamma^{(\tau)}}{1-\tau} - \frac{\tau}{n(1-\tau)} \mu_i, \quad i = 1, \dots, n,$$

where  $\mu_i$  is the corresponding eigenvalues of  $(P^{(\tau)})^{-1}$ . Therefore, it holds

$$L_\tau = \min_i \lambda_i = \frac{\gamma^{(\tau)}}{1-\tau} - \frac{\tau}{n(1-\tau)} \lambda_{\max}((P^{(\tau)})^{-1}),$$

which proves part (i).

For part (ii), if  $P^* \succ 0$ , then  $\lambda_{\min}(P^{(\tau_k)}) \rightarrow \lambda_{\min}(P^*) > 0$  and hence  $\lambda_{\max}((P^{(\tau_k)})^{-1})$  stays bounded. Since  $\tau_k/(1-\tau_k) \rightarrow 0$ , it holds

$$\Delta_{\tau_k} = \frac{\tau_k}{n(1-\tau_k)} \lambda_{\max}((P^{(\tau_k)})^{-1}) \rightarrow 0.$$

We complete the proof.  $\square$

**Remark.** The condition that the subsequential limit  $P^*$  satisfies  $P^* \succ 0$  in Theorem 12 is mathematically strong, but it can be relaxed. Indeed, the tightness requirement there only involves the product

$$\frac{\tau}{1-\tau} \lambda_{\max}((P^{(\tau)})^{-1}),$$

and asymptotic tightness follows whenever this quantity vanishes as  $\tau \downarrow 0$ , namely,

$$\lim_{\tau \downarrow 0} \frac{\tau}{1-\tau} \lambda_{\max}((P^{(\tau)})^{-1}) = 0.$$

Thus, strict positivity of the limiting matrix  $P^*$  is not required. It suffices that  $\lambda_{\max}((P^{(\tau)})^{-1})$  grows more slowly than  $1/\tau$  as  $\tau \downarrow 0$ , such that the decay of  $\tau$  dominates the growth of  $\lambda_{\max}((P^{(\tau)})^{-1})$ . In general, this relaxed condition is mild: for sufficiently small  $\tau$ , the product  $\tau \lambda_{\max}((P^{(\tau)})^{-1})$  can be numerically small in practice. Actually, as documented in Section 6, this relaxed condition is satisfied across all 25 diverse numerical experiments reported in this paper.

### 5.3 Regularized Normalized Value Iteration

Having established the existence of regularized fixed points in Theorem 7, we now turn to a practical procedure for computing them. We propose a *regularized normalized value iteration* (RNDI), a fixed-point scheme for solving fixed-point problem  $\widehat{\Phi}_\tau(P^{(\tau)}) = P^{(\tau)}$ .

Given  $\tau \in (0, 1)$  and an initial  $P_0 \in \mathbb{S}_{++}^n$  with  $\text{Tr } P_0 = 1$ , define the iteration

$$P_{k+1} := \widehat{\Phi}_\tau(P_k), \quad k \in \mathbb{N}.$$

We next derive explicit constants leading to a global contraction condition and, consequently, to linear convergence. The next result bounds the Lipschitz constant of  $\Phi$  on interior slices, which is the key step toward a contraction argument.

**Lemma 4.** Let  $a > 0$  and define  $c_R(a) := (a \lambda_{\min}(R_0))^{-1}$ . Then, for any  $P, Q \in \mathcal{S}_a := \{X \in \mathbb{S}_{++}^n : X \succeq aI, \text{Tr } X = 1\}$ , it holds

$$\|\Phi(P) - \Phi(Q)\| \leq L_\Phi(a) \|P - Q\|, \quad L_\Phi(a) := \alpha_A + 2\alpha_S^2 c_R(a) + \alpha_S^2 \alpha_R c_R(a)^2.$$

Moreover,

$$\sup_{P \in \mathcal{S}_a} \|\Phi(P)\| \leq C_\Phi(a) := \alpha_A + \alpha_S^2 c_R(a)$$

holds.

*Proof.* For any  $a > 0$  and let  $P, Q \in \mathcal{S}_a := \{X \succeq aI, \text{Tr } X = 1\}$ . First observe that

$$R(P) \succeq aR_0 \Rightarrow \|R(P)^{-1}\| \leq c_R(a) := \frac{1}{a \lambda_{\min}(R_0)}$$

and the same holds for  $R(Q)^{-1}$ . We also use the elementary bounds

$$\|S(P) - S(Q)\| \leq \alpha_S \|P - Q\|, \quad \|R(P) - R(Q)\| \leq \alpha_R \|P - Q\|.$$

Moreover, since  $P, Q \succeq 0$  and  $\text{Tr } P = \text{Tr } Q = 1$ , we have  $\|P\| \leq 1$  and  $\|Q\| \leq 1$ . Hence, it holds

$$\|S(P)\| \leq \alpha_S \|P\| \leq \alpha_S, \quad \|S(Q)\| \leq \alpha_S.$$

Decompose

$$\Phi(P) - \Phi(Q) = \underbrace{A^\top (P - Q)A + \sigma^2 \bar{A}^\top (P - Q)\bar{A}}_{(\text{I})} - \underbrace{\left( S(P)R(P)^{-1}S(P)^\top - S(Q)R(Q)^{-1}S(Q)^\top \right)}_{(\text{II})}.$$

The affine part (I) is bounded by

$$\|A^\top (P - Q)A + \sigma^2 \bar{A}^\top (P - Q)\bar{A}\| \leq \alpha_A \|P - Q\|.$$

For the nonlinear part (II), insert and subtract intermediate terms to obtain

$$\begin{aligned} & S(P)R(P)^{-1}S(P)^\top - S(Q)R(Q)^{-1}S(Q)^\top \\ = & \underbrace{(S(P) - S(Q))R(P)^{-1}S(P)^\top}_{(\text{II.a})} + \underbrace{S(Q)(R(P)^{-1} - R(Q)^{-1})S(P)^\top}_{(\text{II.b})} \\ & + \underbrace{S(Q)R(Q)^{-1}(S(P) - S(Q))^\top}_{(\text{II.c})}. \end{aligned}$$

Taking norms and using  $\|XY\| \leq \|X\|\|Y\|$  yield

$$\|(\text{II.a})\| \leq \|S(P) - S(Q)\| \|R(P)^{-1}\| \|S(P)\| \leq \alpha_S c_R(a) \alpha_S \|P - Q\| = \alpha_S^2 c_R(a) \|P - Q\|,$$

$$\|(\text{II.c})\| \leq \|S(Q)\| \|R(Q)^{-1}\| \|S(P) - S(Q)\| \leq \alpha_S c_R(a) \alpha_S \|P - Q\| = \alpha_S^2 c_R(a) \|P - Q\|.$$

For (II.b), note that

$$R(P)^{-1} - R(Q)^{-1} = R(P)^{-1} (R(Q) - R(P)) R(Q)^{-1},$$

thus it holds

$$\|R(P)^{-1} - R(Q)^{-1}\| \leq \|R(P)^{-1}\| \|R(Q) - R(P)\| \|R(Q)^{-1}\| \leq c_R(a)^2 \alpha_R \|P - Q\|.$$

Therefore, we get

$$\|(\text{II.b})\| \leq \|S(Q)\| \|R(P)^{-1} - R(Q)^{-1}\| \|S(P)\| \leq \alpha_S (c_R(a)^2 \alpha_R) \alpha_S \|P - Q\| = \alpha_S^2 \alpha_R c_R(a)^2 \|P - Q\|.$$

Collecting the three bounds (II.a)-(II.c) and adding the affine part (I), we obtain

$$\|\Phi(P) - \Phi(Q)\| \leq \left( \alpha_A + 2\alpha_S^2 c_R(a) + \alpha_S^2 \alpha_R c_R(a)^2 \right) \|P - Q\| = L_\Phi(a) \|P - Q\|.$$

Therefore, for any  $P \in \mathcal{S}_a$ , we have

$$\|\Phi(P)\| \leq \|A^\top PA + \sigma^2 \bar{A}^\top P\bar{A}\| + \|S(P)R(P)^{-1}S(P)^\top\| \leq \alpha_A + \alpha_S^2 c_R(a) =: C_\Phi(a).$$

This establishes both bounds and completes the proof.  $\square$

We can now control the Lipschitz constant of the regularized normalized operator  $\widehat{\Phi}_\tau$ .

**Theorem 13.** *Fix  $\tau \in (0, 1)$  and let  $\delta_\tau$  be as in (18). For all  $P, Q \in \mathcal{S}_{\delta_\tau} = \{X \in \mathbb{S}_{++}^n : X \succeq \delta_\tau I, \text{Tr}(X) = 1\}$ , it holds*

$$\|\widehat{\Phi}_\tau(P) - \widehat{\Phi}_\tau(Q)\| \leq \Lambda(\tau) \|P - Q\|$$

with the constant

$$\Lambda(\tau) := \frac{(1 - \tau) L_\Phi(\delta_\tau)}{\tau} + \frac{(1 - \tau) ((1 - \tau) C_\Phi(\delta_\tau) + \frac{\tau}{n}) n L_\Phi(\delta_\tau)}{\tau^2},$$

where  $L_\Phi$  and  $C_\Phi$  are defined in Lemma 4. If  $\Lambda(\tau) < 1$ , the following statements are equivalent.

- i)  $\widehat{\Phi}_\tau$  is a contraction mapping on  $(\mathcal{S}_{\delta_\tau}, \|\cdot\|)$ .
- ii) There exists a unique fixed point  $P^{(\tau)} \in \mathcal{S}_{\delta_\tau}$  with  $\widehat{\Phi}_\tau(P^{(\tau)}) = P^{(\tau)}$ .
- iii) The sequence  $(P_k)_{k \in \mathbb{N}}$  generated by RNNVI converges globally and linearly to  $P^{(\tau)}$ :

$$\|P_k - P^{(\tau)}\| \leq \Lambda(\tau)^k \|P_0 - P^{(\tau)}\| \quad k \in \mathbb{N}.$$

*Proof.* Note that

$$\widehat{\Phi}_\tau(P) - \widehat{\Phi}_\tau(Q) = \frac{Y_\tau(P)}{\text{Tr } Y_\tau(P)} - \frac{Y_\tau(Q)}{\text{Tr } Y_\tau(Q)}, \quad Y_\tau(\cdot) = (1 - \tau)\Phi(\cdot) + \tau \frac{I}{n}.$$

For any positive semi-definite matrices  $Y_\tau(P), Y_\tau(Q)$ ,

$$\left\| \frac{Y_\tau(P)}{\text{Tr } Y_\tau(P)} - \frac{Y_\tau(Q)}{\text{Tr } Y_\tau(Q)} \right\| \leq \frac{\|Y_\tau(P) - Y_\tau(Q)\|}{\nu} + \frac{\max\{\|Y_\tau(P)\|, \|Y_\tau(Q)\|\}}{\nu^2} |\text{Tr}(Y_\tau(P) - Y_\tau(Q))|$$

holds with  $\nu := \inf \text{Tr } Y_\tau(\cdot) \geq \tau$  on  $\mathcal{S}_{\delta_\tau}$ . By Lemma 4, we have

$$\|Y_\tau(P) - Y_\tau(Q)\| = (1 - \tau) \|\Phi(P) - \Phi(Q)\| \leq (1 - \tau) L_\Phi(\delta_\tau) \|P - Q\|,$$

and

$$|\text{Tr}(Y_\tau(P) - Y_\tau(Q))| \leq n \|Y_\tau(P) - Y_\tau(Q)\|.$$

Moreover, it holds

$$\|Y_\tau(\cdot)\| \leq (1 - \tau) C_\Phi(\delta_\tau) + \frac{\tau}{n}$$

on  $\mathcal{S}_{\delta_\tau}$ . Combine these to obtain the stated  $\Lambda(\tau)$ . If  $\Lambda(\tau) < 1$ , Banach's fixed-point theorem (see, e.g., Theorem 8.1.2 of [Borwein and Lewis \(2006\)](#)) gives (i)–(iii).  $\square$

**Remark.** The condition  $\Lambda(\tau) < 1$  is a sufficient (but not necessary) criterion. In particular, since  $\Lambda(\tau) \rightarrow 0$  as  $\tau \uparrow 1$ , there always exists  $\tau_0$  close to 1 such that  $\Lambda(\tau_0) < 1$ .

**Lemma 5.** Fix a trace-normalized interior slice

$$S_a := \{X \in \mathbb{S}_{++}^n : X \succeq aI, \text{Tr } X = 1\}, \quad a > 0.$$

For  $\tau \in (0, 1)$ , let  $\widehat{\Phi}_\tau$  be defined by (7). Then, the mapping

$$(P, \tau, H) \mapsto D\widehat{\Phi}_\tau(P)[H]$$

is jointly continuous on  $S_a \times (0, 1) \times \{H : \|H\| = 1\}$ . Consequently, the local Lipschitz modulus

$$\text{Lip}(P, \tau) := \|D\widehat{\Phi}_\tau(P)\| = \sup_{\|H\|=1} \|D\widehat{\Phi}_\tau(P)[H]\|$$

depends continuously on  $(P, \tau) \in S_a \times (0, 1)$ .

*Proof.* On  $S_a$ ,  $R(P) = B^\top PB + \sigma^2 \bar{B}^\top P \bar{B}$  satisfies  $R(P) \succeq aR_0 \succ 0$ ; hence,  $R(P)^{-1}$  depends continuously on  $P$ . Direct differentiation of (13) yields

$$\begin{aligned} D\Phi(P)[H] &= A^\top HA + \sigma^2 \bar{A}^\top H \bar{A} - (A^\top HB + \sigma^2 \bar{A}^\top H \bar{B})R(P)^{-1}S(P)^\top \\ &\quad - S(P)R(P)^{-1}(B^\top HA + \sigma^2 \bar{B}^\top H \bar{A}) + S(P)R(P)^{-1}(B^\top HB + \sigma^2 \bar{B}^\top H \bar{B})R(P)^{-1}S(P)^\top, \end{aligned}$$

an affine function of  $H$  whose coefficients depend continuously on  $P$ . Thus,  $(P, H) \mapsto D\Phi(P)[H]$  is continuous.

For  $Y_\tau(P) = (1 - \tau)\Phi(P) + \frac{\tau}{n}I$  and  $s_\tau(P) = \text{Tr } Y_\tau(P)$ , we have

$$D\widehat{\Phi}_\tau(P)[H] = \frac{1 - \tau}{s_\tau(P)} \left( D\Phi(P)[H] - \widehat{\Phi}_\tau(P) \text{Tr}(D\Phi(P)[H]) \right),$$

where  $(P, \tau) \mapsto s_\tau(P)$  and  $(P, \tau) \mapsto \widehat{\Phi}_\tau(P)$  are continuous. Hence, the trivariate map

$$(P, \tau, H) \mapsto D\widehat{\Phi}_\tau(P)[H]$$

is continuous on  $S_a \times (0, 1) \times \{H : \|H\| = 1\}$ .

For fixed  $(P, \tau)$ ,  $D\widehat{\Phi}_\tau(P)$  is linear in  $H$ . Since the unit sphere  $\{H : \|H\| = 1\}$  is compact and the above trivariate map is continuous, Berge's maximum theorem (see Berge (1963), p.115, Theorem 1) implies that

$$(P, \tau) \mapsto \text{Lip}(P, \tau) = \sup_{\|H\|=1} \|D\widehat{\Phi}_\tau(P)[H]\|$$

is continuous on  $S_a \times (0, 1)$ . □

The continuity of the local Lipschitz modulus established in Lemma 5 allows us to track the fixed points along a decreasing sequence of  $\tau$ , which is the essence of the continuation method formalized below.

**Theorem 14.** *Suppose  $\tau_0 \in (0, 1)$  satisfies  $\Lambda(\tau_0) < 1$ . Then, one can construct a strictly decreasing sequence of parameters*

$$\tau_0 > \tau_1 > \tau_2 > \dots,$$

together with associated fixed points  $\{P^{(\tau_j)}\}_{j \geq 0}$  of (21), such that at each stage the sequence generated by RNI with parameter  $\tau_{j+1}$ , initialized at  $P^{(\tau_j)}$ , converges locally to  $P^{(\tau_{j+1})}$ . In particular, the continuation procedure produces a decreasing family of parameters  $\{\tau_j\}$  and fixed points  $\{P^{(\tau_j)}\}$  linked by local RNI convergence.

*Proof.* Let  $\tau_0 \in (0, 1)$  be such that  $\Lambda(\tau_0) < 1$ , and fix a target  $\tau \in (0, \tau_0)$ . By Lemma 5, the local Lipschitz modulus  $\text{Lip}(P, \tau)$  depends continuously on  $(P, \tau)$  on  $S_a \times (0, 1)$ . We construct a decreasing sequence  $\{\tau_j\}$  inductively. For  $j = 0$ , note that

$$\text{Lip}(P^{(\tau_0)}, \tau_0) < 1.$$

At step  $j$ , suppose  $\tau_j$  has been chosen and

$$\text{Lip}(P^{(\tau_j)}, \tau_j) < 1$$

holds. By the continuity of  $\text{Lip}(P, \tau)$  at  $(P^{(\tau_j)}, \tau_j)$ , there exists  $\Delta\tau_j > 0$  such that for every  $\tilde{\tau} \in (\tau_j - \Delta\tau_j, \tau_j]$ ,

$$\text{Lip}(P^{(\tau_j)}, \tilde{\tau}) < 1$$

holds and consequently  $\widehat{\Phi}_{\tilde{\tau}}$  is a contraction in a neighborhood of  $P^{(\tau_j)}$ .

Choose

$$\tau_{j+1} \in (\max\{\tau, \tau_j - \Delta\tau_j\}, \tau_j).$$

---

**Algorithm 1** Regularized Normalized Value Iteration

---

**Input:** System matrices  $(A, \bar{A}, B, \bar{B})$ ; noise  $\omega_k \sim \mathcal{N}(0, \sigma^2)$ ; initial  $P_0 \succ 0$  with  $\text{Tr}(P_0) = 1$ ; decreasing schedule  $\tau_0 > \tau_1 > \dots > \tau_M$ ; tolerance  $\varepsilon$ .

**Output:** The tightest certified bounds for the optimal stabilizing rate, together with the parameters at which the best lower and upper bounds are attained and the associated gains.

```

1:  $P \leftarrow P_0$ 
2:  $J_{\text{low}}^{\text{best}} \leftarrow -\infty$ ,  $J_{\text{up}}^{\text{best}} \leftarrow +\infty$ 
3:  $\tau_{\text{low}} \leftarrow \text{None}$ ,  $\tau_{\text{up}} \leftarrow \text{None}$ ,  $K_{\text{up}} \leftarrow \text{None}$ 
4: for  $j = 0, 1, \dots, M$  do
5:    $\tau \leftarrow \tau_j$ ,  $P^{(0)} \leftarrow P$ 
6:   for  $k = 0, 1, 2, \dots$  do
7:      $P^{(k+1)} \leftarrow \frac{(1-\tau)\Phi(P^{(k)}) + \frac{\tau}{n}I}{\text{Tr}((1-\tau)\Phi(P^{(k)}) + \frac{\tau}{n}I)}$ 
8:     if  $\|P^{(k+1)} - P^{(k)}\|_F \leq \varepsilon$  then
9:       break
10:    end if
11:   end for
12:    $P^{(\tau)} \leftarrow P^{(k+1)}$ 
13:    $K^{(\tau)} \leftarrow R(P^{(\tau)})^{-1}S(P^{(\tau)})^\top$ 
14:    $\gamma^{(\tau)} \leftarrow \text{Tr}((1-\tau)\Phi(P^{(\tau)}) + \frac{\tau}{n}I)$ 
15:    $L(P^{(\tau)}) \leftarrow \lambda_{\min}((P^{(\tau)})^{-1/2}\Phi(P^{(\tau)})(P^{(\tau)})^{-1/2})$ 
16:    $J_{\text{low}} \leftarrow \log L(P^{(\tau)})$ ,  $J_{\text{up}} \leftarrow \log\left(\frac{\gamma^{(\tau)}}{1-\tau}\right)$ 
17:   if  $J_{\text{low}} > J_{\text{low}}^{\text{best}}$  then
18:      $J_{\text{low}}^{\text{best}} \leftarrow J_{\text{low}}$ ,  $\tau_{\text{low}} \leftarrow \tau$ 
19:   end if
20:   if  $J_{\text{up}} < J_{\text{up}}^{\text{best}}$  then
21:      $J_{\text{up}}^{\text{best}} \leftarrow J_{\text{up}}$ ,  $\tau_{\text{up}} \leftarrow \tau$ ,  $K_{\text{up}} \leftarrow K^{(\tau)}$ 
22:   end if
23:    $P \leftarrow P^{(\tau)}$ 
24: end for
25: Return:  $J^* \in [J_{\text{low}}^{\text{best}}, J_{\text{up}}^{\text{best}}]$ ,  $\rho^* \in [e^{J_{\text{low}}^{\text{best}}/2}, e^{J_{\text{up}}^{\text{best}}/2}]$ ,
26: corresponding parameters  $(\tau_{\text{low}}, \tau_{\text{up}})$  and gain  $K_{\text{up}}$ .

```

---

Since  $\delta_\tau$  is strictly increasing in  $\tau$ , we have  $\mathcal{S}_{\delta_{\tau_j}} \subset \mathcal{S}_{\delta_{\tau_{j+1}}}$  whenever  $\tau_{j+1} < \tau_j$ . Hence  $P^{(\tau_j)} \in \mathcal{S}_{\delta_{\tau_{j+1}}}$  and is a valid initialization for RNVI at parameter  $\tau_{j+1}$ .

Because  $\widehat{\Phi}_{\tau_{j+1}}$  is a contraction near  $P^{(\tau_j)}$ , the sequence generated by RNVI with parameter  $\tau_{j+1}$ , initialized at  $P^{(\tau_j)}$ , converges locally to the fixed point  $P^{(\tau_{j+1})}$ . This yields

$$\text{Lip}(P^{(\tau_{j+1})}, \tau_{j+1}) < 1,$$

allowing the induction to proceed.

In this manner, one obtains a decreasing sequence  $\{\tau_j\}$  with local convergence at each stage, and the continuation procedure produces the fixed point  $P^{(\tau)}$ .  $\square$

**Remark.** The fixed point of (21) is known to exist by Brouwers fixed-point theorem, but that theorem is nonconstructive: it does not explain how to obtain an actual fixed point in practice. The continuation result in Theorem 14 addresses this gap by providing a problem-specific mechanism that produces a decreasing family  $\{\tau_j\}$  together with associated fixed points  $\{P^{(\tau_j)}\}$ , each obtained by locally convergent RNVI iteration starting from the preceding stage. Its limitation is that it does not guarantee that an arbitrarily prescribed target value of  $\tau$  can be reached along such a path.

As an alternative, one may resort to constructive methods based on Sperner-type simplicial subdivision for a continuous self-map  $F : K \rightarrow K$  on a compact convex set. By refining a simplicial mesh of  $K$  and labeling each vertex according to the direction of  $F(x) - x$ , Sperner's lemma ensures the existence of a fully labelled small simplex; points within this simplex provide approximate fixed points with accuracy proportional to the mesh size.

Having established global convergence under a contraction condition and local convergence via continuation, we summarize the complete scheme in Algorithm 1. The algorithm couples RNVI with the certified bounds for  $\rho^*$  from Theorem 11.

**Relation to Riccati theory and numerical methods.** Equation (21) can be viewed algebraically as a Riccati-type nonlinear matrix equation on  $\mathbb{S}_{++}^n$ , since  $\Phi$  has a structure analogous to generalized Riccati operators in discrete-time stochastic LQ problems with multiplicative noise. Nevertheless, its role here differs from classical LQ Riccati equations.

*Classical Riccati theory and numerical methods.* In continuous- and discrete-time LQ control, algebraic Riccati equations (AREs) characterize optimal regulators and stabilizing feedback gains under standard stabilizability/detectability assumptions; see [Anderson and Moore \(2007\)](#); [Bittanti et al. \(1991\)](#). This structure supports, among others: (i) Hamiltonian/symplectic methods based on stable invariant subspaces [Laub \(1979\)](#); (ii) Newton–Kleinman iterations solving a Lyapunov equation at each step [Feitzinger et al. \(2009\)](#); and (iii) projection/Krylov large-scale solvers [Bunse-Gerstner \(1996\)](#).

*Why do these methods not apply directly in our setting?* Although  $\Phi$  is Riccati-type in form, our problem is a Bellman-type nonlinear eigenvalue problem  $\Phi(P) = \gamma P$ , and the regularization in (21) is essential. Accordingly,  $\hat{\Phi}_\tau(P) = P$  is not a standard ARE; there is no associated Hamiltonian matrix for symplectic solvers; and trace normalization breaks the Loewner-order monotonicity used in many Riccati iterations. Hence we instead rely on the contraction framework in Theorem 13, which provides a direct and rigorous basis for RNVI.

*Future directions.* The order structure of  $P \mapsto \Phi(P)$  suggests possible links to nonlinear Perron–Frobenius theory and Hilbert's projective metric [Lemmens and Nussbaum \(2012\)](#). Developing cone-theoretic uniqueness results or dynamical-systems interpretations (e.g., generalized Riccati flows) may yield stronger guarantees beyond contractivity.

## 6 Numerical Experiments

We now demonstrate the proposed framework through two representative numerical examples. The first examines how the optimal stabilizing rate responds to varying noise intensities, while the second explores a higher-dimensional case that is highly challenging to stabilize, thus it is not clear a priori whether this system can be stabilized in the mean-square sense.

### 6.1 Two-dimensional system: noise-level sweep

**Setup.** We first consider a stabilizable two-dimensional stochastic system

$$x_{k+1} = (A + \bar{A}\omega_k)x_k + (B + \bar{B}\omega_k)u_k, \quad \omega_k \sim \mathcal{N}(0, \sigma^2)$$

with

$$A = \begin{bmatrix} 0.88 & 0.22 \\ -0.18 & 0.86 \end{bmatrix}, \quad \bar{A} = \begin{bmatrix} 0.12 & 0.04 \\ 0.06 & 0.10 \end{bmatrix}, \quad B = \begin{bmatrix} 1.0 \\ 0.7 \end{bmatrix}, \quad \bar{B} = \begin{bmatrix} 0.20 \\ 0.25 \end{bmatrix}.$$

We sweep the noise intensity

$$\sigma \in \{1.00, 1.50, 2.00, 3.00\}.$$

For each  $\sigma$ , RNNI is executed over a decreasing logarithmic grid  $\tau \in [0.5, 10^{-5}]$ , started from the previous fixed point  $P^{(\tau_{\text{prev}})}$ .

**Methodology.** Following the construction in Section 5, each RNNI fixed point  $P^{(\tau)}$  provides computable bounds on the asymptotic growth rate:

$$\underline{J}(\tau) = \log L(P^{(\tau)}), \quad \bar{J}(\tau) = \log \left( \frac{\gamma^{(\tau)}}{1-\tau} \right).$$

To extract the tightest certified bounds, we take the pointwise best bounds across  $\tau$ :

$$J_{\text{low}}^{\text{best}} = \max_{\tau} \underline{J}(\tau), \quad J_{\text{up}}^{\text{best}} = \min_{\tau} \bar{J}(\tau).$$

Since  $J^* = 2 \log \rho^*$ , these bounds immediately yield an interval for  $\rho^*$ . Theorem 12 shows that the tightness of the RNNI certificates is governed by the squared gap

$$\Delta_{\tau} = \frac{\tau}{n(1-\tau)} \lambda_{\max}(P^{(\tau)-1}).$$

This motivates a numerical inspection of how  $\Delta_{\tau}$  behaves as  $\tau \downarrow 0$ , and whether the matrices  $P^{(\tau)}$  remain well conditioned.

Motivated by Theorem 12 and Remark 5.2, we therefore include two additional diagnostic plots: (i) the squared-gap curve  $\Delta_{\tau}$ , and (ii) the conditioning measure  $\lambda_{\max}((P^{(\tau)})^{-1}) = 1/\lambda_{\min}(P^{(\tau)})$ , both plotted across  $\tau$  for all noise levels  $\sigma$ . The first plot directly illustrates the decay of the certified squared gap as  $\tau$  decreases, while the second provides a numerical indication of whether the relaxed tightness condition in Remark 5.2 is plausibly satisfied over the explored range of  $\tau$ .

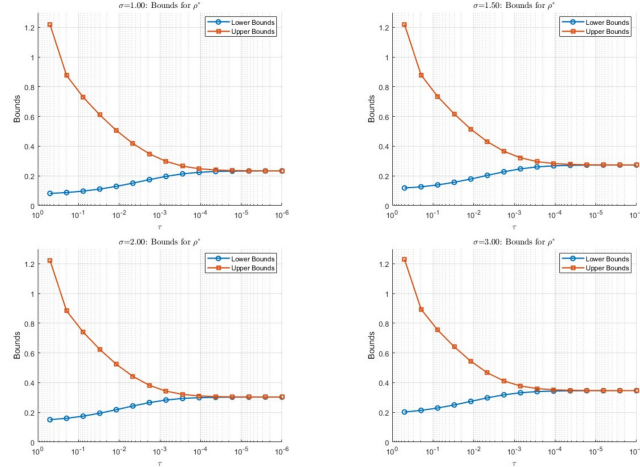


Figure 1: Bounds for  $\rho^*$  over the  $\tau$ -grid for different noise levels  $\sigma$ .

In addition, for each noise level  $\sigma$  we also record the number of RNNI iterations required for convergence at every value of  $\tau$ .

**Results.** Figure 1 shows, for each noise level  $\sigma$ , the lower (blue) and upper (red) bounds for  $\rho^*$  across the  $\tau$ -grid which decreasing to the right. Table 1 then summarizes the best bounds across  $\tau$ , and reports the corresponding intervals for both  $J^*$  and  $\rho^*$ .

Figures 2–3 reveal two important and consistent phenomena:

1. The certified squared-gap  $\Delta_{\tau}$  decreases rapidly as  $\tau$  becomes small for all noise levels  $\sigma$ . Numerically,  $\Delta_{\tau}$  is already below  $10^{-2}$  once  $\tau \approx 10^{-3}$ , and its decay is consistent with the qualitative trend described by Theorem 12.

Table 1: Best Bounds for  $J^*$  and  $\rho^*$  in the two-dimensional system

$\sigma$	$J_{\text{low}}^{\text{best}}$	$J_{\text{up}}^{\text{best}}$	bounds for $\rho^*$
1.0	-2.9170	-2.8963	[ 0.2320 , 0.2350 ]
1.50	-2.5979	-2.5867	[ 0.2720 , 0.2740 ]
2.00	-2.3896	-2.3822	[ 0.3020 , 0.3030 ]
3.00	-2.1205	-2.1200	[ 0.3459 , 0.3467 ]

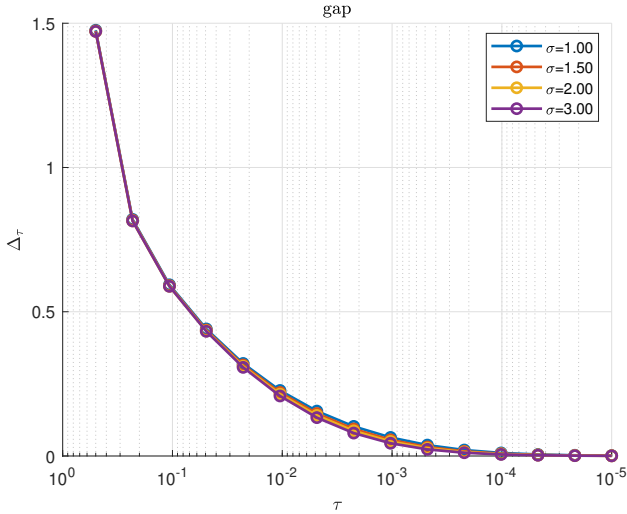


Figure 2: Certified squared-gap  $\Delta_\tau = \frac{\tau}{n(1-\tau)} \lambda_{\max}((P^{(\tau)})^{-1})$  for each noise level  $\sigma$ .

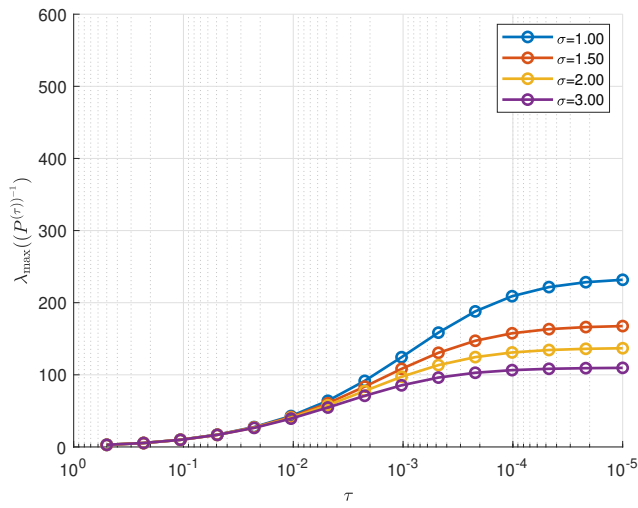


Figure 3:  $\lambda_{\max}((P^{(\tau)})^{-1}) = 1/\lambda_{\min}(P^{(\tau)})$  for each noise level  $\sigma$ .

2.  $\lambda_{\max}((P^{(\tau)})^{-1})$  remains well bounded across  $\sigma$  and across all small  $\tau$ . This behavior supports the relaxed condition stated in Remark 5.2, indicating that no noticeable deterioration occurs as  $\tau$  decreases.

Together, these two diagnostic plots confirm that RNNI produces well-conditioned fixed points near  $\tau = 0$  and that the certified bounds become extremely tight in this regime.

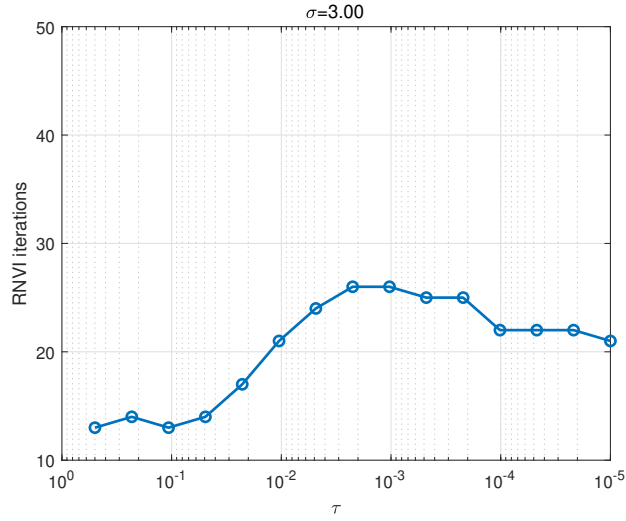


Figure 4: RNVI iteration counts for  $\sigma = 3$  across the  $\tau$ grid.

Figure 4 reports the RNVI iteration count for  $\sigma = 3$  across the  $\tau$ grid. Although the continuation Theorem 14 does not guarantee that an arbitrary preassigned sequence of  $\tau$ values will always lie within the local basin of convergence, the observed behavior is highly stable: the iteration count remains uniformly small (between 12 and 30) over more than five orders of magnitude in  $\tau$ . Finally, we note that for every noise level and every value of  $\tau$  in the sweep, the RNVI iteration converges in only a small number of steps. This rapid convergence is consistently observed not only in this noisesweep experiment but also in all other numerical studies reported later in the paper. To avoid disrupting the flow, we do not tabulate all iteration counts, but the behavior illustrated in Figure 4 is representative of the overall performance.

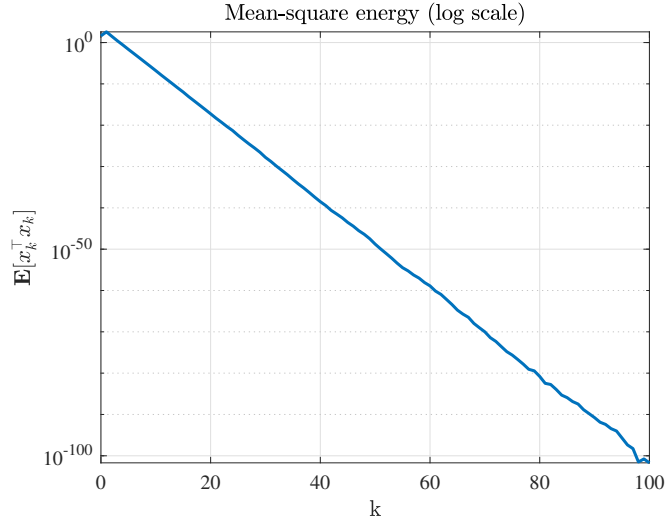


Figure 5: Mean-square energy trajectory in logarithmic scale ( $\sigma = 2$ ).

In addition, we also inspect the closed-loop behavior at the noise level  $\sigma = 2$ . For this case, the tightest certified upper bound in Table 1 is attained at  $\tau = 10^{-5}$ , yielding the feedback gain

$$K_{\text{up}} = [2.1167 \quad -0.8840]$$

which can be regarded as a numerically near-optimal stabilizing gain. To assess its mean-square performance, we simulate the closed-loop system under  $u_k = -K_{\text{up}}x_k$  with deterministic initial condition  $x_0 = (5, -4)^\top$ , and approximate  $\mathbb{E}[x_k^\top x_k]$  by averaging over  $10^4$  trajectories. The resulting curve (Fig. 5) is nearly a straight line on a logarithmic scale, exhibiting a clear exponential decay of the form  $\mathbb{E}[x_k^\top x_k]$ . This confirms that the RNVI-generated gain achieves exponential mean-square stabilization even under relatively strong multiplicative noise.

**Discussion.** The results highlight two consistent features. First, as the noise intensity  $\sigma$  increases, the certified optimal stabilizing rate  $\rho^*$  becomes larger, reflecting the expected degradation of mean-square stability under stronger multiplicative disturbances. Second, the certified gaps remain very small, on the order of  $10^{-3} \sim 10^{-2}$  for  $\rho^*$ . This tightness demonstrates that RNVI yields not only reliable existence and convergence guarantees but also numerically precise performance bounds across a wide range of noise levels.

Figures 2–3 illustrate the behavior of the quantity  $\tau \lambda_{\max}((P^{(\tau)})^{-1})$  as  $\tau \downarrow 0$ . In all cases considered, this product remains small for sufficiently small  $\tau$ , leading to a rapid decay of the certified squared-gap  $\Delta_\tau$ . These observations are fully consistent with the relaxed tightness condition discussed in Remark 5.2, and indicate that the sufficient condition in Theorem 12 (ii) is, at least numerically, not restrictive in the present setting.

For illustration, we also inspect the closed-loop behavior at  $\sigma = 2$  using the RNVI-derived approximate optimal gain. A Monte Carlo simulation shows that  $\mathbb{E}[x_k^\top x_k]$  decays nearly linearly on a logarithmic scale, indicating clear exponential mean-square stabilization under this feedback.

## 6.2 Four-Dimensional System Near the Stability Boundary

This example consists of two complementary parts. First, we examine a single near-marginal instance for which it is not clear *a priori* whether mean-square stabilization is possible; the RNVI framework confirms that this instance is indeed stabilizable and provides tight, verifiable bounds for its optimal stabilizing rate. Second, we perform a *scaling experiment across the stability boundary* to study how the certified bounds evolve as the system gradually transitions from the strictly stable region to the unstable regime.

### 6.2.1 Single Near-Marginal Instance

**Setup.** We consider a four-dimensional stochastic system with  $\sigma = 2$ ,

$$A = \begin{bmatrix} 0.9999 & 0.34 & 0 & 0 \\ 0 & 0.9996 & 0.25 & 0 \\ 0 & 0 & 0.9992 & 0.22 \\ 0 & 0 & 0 & 0.9988 \end{bmatrix}, \quad \bar{A} = \begin{bmatrix} 0.16 & 0.06 & 0 & 0 \\ 0.05 & 0.13 & 0.05 & 0 \\ 0 & 0.04 & 0.11 & 0.05 \\ 0 & 0 & 0.03 & 0.10 \end{bmatrix},$$

$$B = \begin{bmatrix} 0.0024 & 0 \\ 0 & 0.05 \\ 0.22 & 0 \\ 0 & 0.14 \end{bmatrix}, \quad \bar{B} = \begin{bmatrix} 0.375 & 0 \\ 0 & 0.25 \\ 0.15 & 0 \\ 0 & 0.15 \end{bmatrix}.$$

Stabilizing this system is challenging, due to the following features.

1. The noisefree, uncontrolled part of the system already lies at the boundary of stability, since  $A$  has eigenvalues very close to one, and even weak multiplicative noise can readily push the overall dynamics into an unstable regime.
2. The input matrices  $B$  and  $\bar{B}$  contain many zero entries. Several state coordinates, especially those associated with the weakest modes of  $A$ , receive very limited actuation. As a result, the

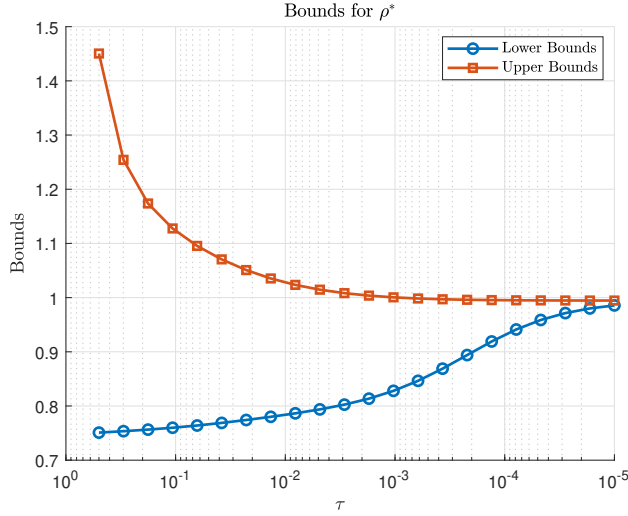


Figure 6: Bounds for  $\rho^*$  over the  $\tau$ -grid for a near-marginally stable example.

controller has little direct authority over exactly the states that require the most stabilization effort.

3. Multiplicative noise is injected precisely in these weakly controlled directions, with additional coupling through  $\bar{A}$ .

Together, these effects make it entirely possible that this system is not mean-square stabilizable, thus the optimal stabilizing rate  $\rho^*$  is not known a priori to be smaller than one and might in fact be arbitrarily close to or even exceed one.

**Results.** For a decreasing logarithmic grid of  $\tau \in [0.5, 10^{-5}]$ , Figure 6 shows the bounds for  $\rho^*$  across  $\tau$  and the best bounds are

$$J^* \in [-0.0290, -0.0109], \quad \rho^* \in [0.9856, 0.9946],$$

achieved at

$$\tau_{\text{low}} = \tau_{\text{up}} = 1 \times 10^{-5}$$

which yields the near-optimal feedback stabilizing gain

$$K_{\text{up}} = \begin{bmatrix} 0.8553 & 2.2097 & 1.5573 & -0.9092 \\ -0.7399 & -1.5910 & -0.3794 & 1.8438 \end{bmatrix}.$$

To further illustrate the closed-loop behavior under this near-optimal gain, we simulate the mean-square evolution of the system with deterministic initial condition  $x_0 = (5, 4, 3, 2)^\top$  and  $u_k = -K_{\text{up}}x_k$ . The quantity  $\mathbb{E}[x_k^\top x_k]$  is approximated by averaging over  $10^4$  i.i.d. trajectories. The resulting curve on a logarithmic scale (Fig. 7) exhibits a clear linear trend with negative slope, demonstrating exponential mean-square decay under the RNNI derived gain.

**Discussion.** This example highlights the effectiveness of our method in a particularly challenging setting: although the system is a priori close to being unstabilizable, our certified bounds establish that  $\rho^* < 1$ , thereby confirming mean-square stabilizability, and the RNNI framework further produces a near-optimal gain  $K_{\text{up}}$  that achieves exponential decay in practice.

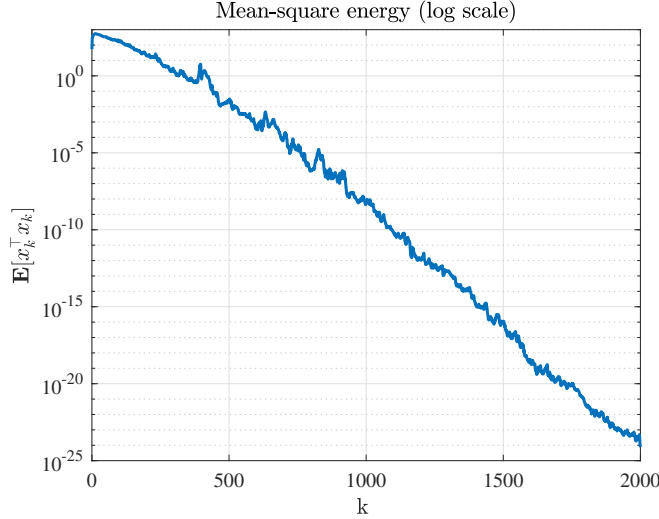


Figure 7: Mean-square energy trajectory in logarithmic scale

### 6.2.2 Scaling Study Across the Stability Boundary

**Objective and Methodology.** To stress-test RNVI beyond a single operating point, we smoothly vary the system across the marginal regime. We introduce a global scaling factor

$$\theta \in [0.95, 1.10]$$

and consider  $A_\theta = \theta A$ , while keeping  $(\bar{A}, \bar{B}, \bar{B}, \sigma)$  fixed. This radial scaling moves the eigenvalues of  $A$  with respect to the unit circle:  $\theta < 1$  pushes them inward (more stable),  $\theta = 1$  recovers the near-marginal instance, and  $\theta > 1$  moves the dynamics beyond the boundary. For each  $\theta$  we run RNVI over a decreasing grid of regularization parameters  $\tau \in [0.5, 10^{-5}]$  and report the tightest *certified bounds* on  $\rho^*$  obtained across the grid.

**Results.** Table 2 summarizes the bounds for  $\rho^*$  at 20 values of  $\theta$ . The corresponding curves and bound width are visualized in Figures 9–10.

Table 2: Bounds for  $\rho^*$  under global scaling  $A_\theta$  in the four-dimensional system

$\theta$	Bounds for $\rho^*$	$\theta$	Bounds for $\rho^*$
0.950	[0.9360, 0.9492]	1.029	[1.0132, 1.0208]
0.958	[0.9441, 0.9564]	1.036	[1.0206, 1.0279]
0.966	[0.9521, 0.9635]	1.045	[1.0281, 1.0351]
0.974	[0.9599, 0.9707]	1.053	[1.0355, 1.0422]
0.981	[0.9677, 0.9778]	1.061	[1.0429, 1.0494]
0.989	[0.9754, 0.9850]	1.068	[1.0503, 1.0566]
0.997	[0.9831, 0.9922]	1.076	[1.0577, 1.0637]
1.005	[0.9907, 0.9993]	1.084	[1.0650, 1.0709]
1.013	[0.9982, 1.0065]	1.092	[1.0723, 1.0780]
1.021	[1.0057, 1.0136]	1.100	[1.0797, 1.0852]

Beyond the bounds themselves, we also monitor the *squared gap*  $\Delta_\tau$ . Figure 8 displays  $\Delta_\tau$  as a function of  $\tau$  for all  $\theta$  on a single plot. For every scaling factor, the curves decay as  $\tau$  decreases and remain of moderate magnitude, indicating that the certified bounds become tighter when approaching the small  $\tau$  regime and that the RNVI fixed points do not exhibit pathological conditioning in this

four-dimensional example.

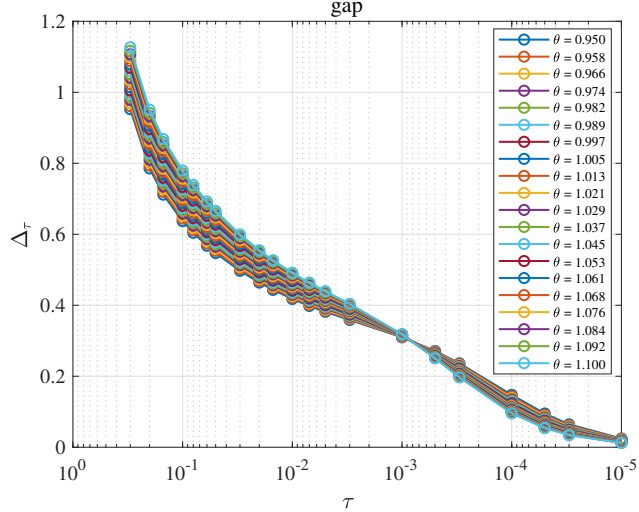


Figure 8: Certified squared-gap  $\Delta_\tau = \frac{\tau}{n(1-\tau)} \lambda_{\max}((P^{(\tau)})^{-1})$  for each  $\theta$ .

For a stabilizable case such as  $\theta_1 = 1.005$ , the tightest certified upper bound on  $\rho^*$  is attained at  $\tau = 10^{-5}$ , yielding the near-optimal feedback stabilizing gain

$$K_1 = \begin{bmatrix} 0.8558 & 2.2192 & 1.5695 & -0.9108 \\ -0.7380 & -1.5940 & -0.3847 & 1.8506 \end{bmatrix}.$$

In contrast, for a nearby parameter value  $\theta_2 = 1.021$ , where the certified interval satisfies  $\rho^* > 1$  and hence stabilization is impossible, the RNNI procedure returns the gain

$$K_2 = \begin{bmatrix} 0.8570 & 2.2475 & 1.6058 & -0.9154 \\ -0.7322 & -1.6023 & -0.4000 & 1.8707 \end{bmatrix}.$$

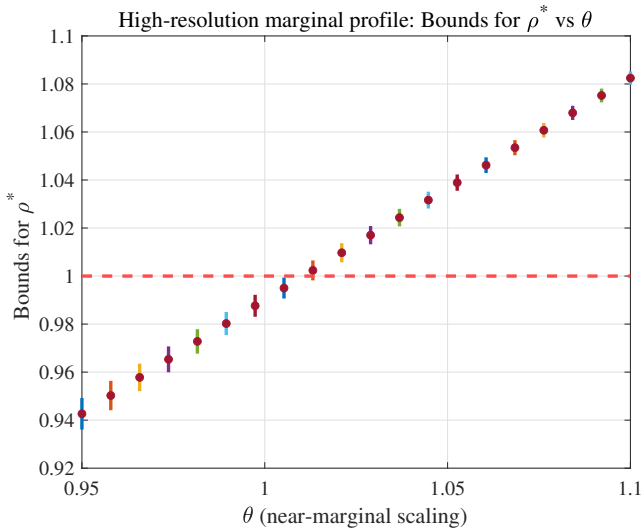


Figure 9: Certified bounds for  $\rho^*$  versus the scaling  $\theta$ .

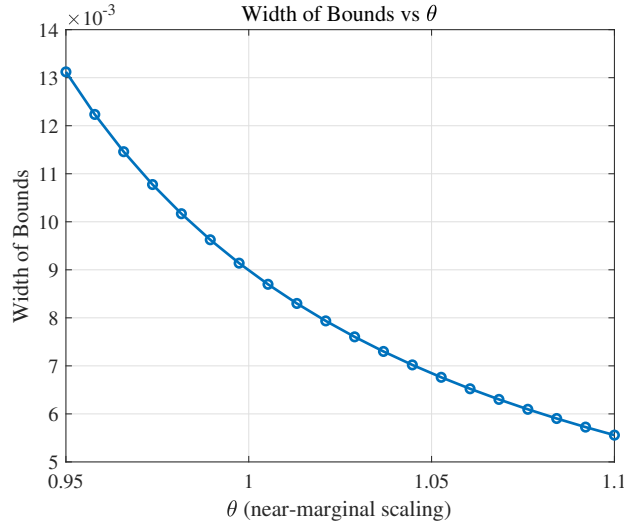


Figure 10: Width of the certified bounds for  $\rho^*$  as a function of  $\theta$ . The width decreases slightly as  $\theta$  increases, corroborating the numerical stability of the RNNI certificates near and beyond the boundary.

**Discussion.** Three points emerge clearly from the scaling study.

1. **Localization of the stability threshold.** For all  $\theta \leq 1.005$ , the certified intervals for  $\rho^*$  lie strictly below one, which rigorously certifies mean-square stabilizability across this entire parameter range. For  $\theta \geq 1.021$ , both bounds exceed one, which rules out mean-square stabilizability and, at the same time, quantifies the minimal exponential growth rate that any admissible controller can achieve (see Tab. 2 and Fig. 9). Taken together, these two regimes localize the stability threshold to a very narrow window around the numerically identified value  $\theta \approx 1.013$ .
2. **Robustness near and beyond the threshold.** As  $\theta$  moves from the clearly stabilizable region into the non-stabilizable one, the certified intervals for  $\rho^*$  vary smoothly and even exhibit a slight reduction in interval width (see Fig. 10). This behavior indicates that the RNNI-based certificates remain numerically well behaved even when the system operates close to the loss of stabilizability or in the unstable regime.
3. **Certification and controller synthesis across operating points.** For each  $\theta$ , RNNI delivers both two-sided bounds on  $\rho^*$  and an associated feedback gain (such as  $K_1$  at  $\theta = 1.005$  and  $K_2$  at  $\theta = 1.021$ ). Thus, the method not only certifies the parameter ranges where mean-square stabilization is achievable, but also provides meaningful candidate feedback laws and quantitative growth rates across the entire spectrum of  $\theta$  values.
4. **Resolution near criticality and decay of the certified gap.** In the near-critical parameter range, where both bounds for  $\rho^*$  are close to one, the certified squared-gap  $\Delta_\tau$  produced by RNNI decreases steadily as  $\tau$  is reduced. This behavior is consistent with the relaxed tightness requirement described in Remark 5.2: for the values of  $\tau$  used in this example, the quantity  $\tau \lambda_{\max}((P^{(\tau)})^{-1})$  remains numerically small, and the resulting certificates sharpen accordingly. Thus, even when the stabilizing rate is very close to the transition between stability and instability, RNNI continues to provide reliable and increasingly tight two-sided bounds as  $\tau$  is refined.

## 7 Conclusion

We develop a quantitative framework for analyzing mean-square exponential stabilization of stochastic systems with multiplicative noise under state-feedback control policies. The study introduces the optimal stabilizing rate  $\rho^*$  as a measure of how fast stabilization can be achieved, and pursues two complementary directions. On one hand, norm-based conditions are extended to the stochastic setting, providing a necessary and sufficient condition for the exact attainability of the optimal stabilizing rate  $\rho^*$  and conservative upper and lower estimates. On the other hand, we reformulate the Problem (OC) into an optimal control Problem (OSR) and developed the RNNI algorithm, obtaining the computable two-sided bounds for the optimal stabilizing rate under any admissible state-feedback control policies.

These results yields both theoretical insights and practical tools for stabilization under multiplicative noise. Future work may extend the framework toward data-driven formulations, robustness against modeling errors, and scalable algorithms for high-dimensional systems.

## References

A. D. Ames, S. Coogan, M. Egerstedt, G. Notomista, K. Sreenath, and P. Tabuada. Control barrier functions: Theory and applications.

B. Anderson and J. Moore. *Linear Optimal Control*. Prentice-Hall International Inc., 1971.

B. D. O. Anderson and J. B. Moore. *Optimal control: linear quadratic methods*. Courier Corporation, 2007.

B. Bamieh and M. Filo. An inputoutput approach to structured stochastic uncertainty. *IEEE Transactions on Automatic Control*, 65(12):5012–5027, 2020.

C. Berge. *Topological spaces: Including a treatment of multi-valued functions, vector spaces and convexity*. Oliver & Boyd, 1963.

S. Bittanti, A. J. Laub, and J. C. Willems. *The Riccati Equation*. Springer, 1991.

G. Blankenship. Stability of linear differential equations with random coefficients. *IEEE Transactions on Automatic Control*, 22(5):834–838, 1977.

J. Borwein and A. Lewis. *Convex Analysis and Nonlinear Optimization: Theory and Examples*. Springer, 2006.

S. Boyd, L. El Ghaoui, E. Feron, and V. Balakrishnan. *Linear matrix inequalities in system and control theory*. SIAM, 1994.

S. P. Boyd and L. Vandenberghe. *Convex optimization*. Cambridge university press, 2004.

H. Brezis. *Functional analysis, Sobolev spaces and partial differential equations*, volume 2. Springer, 2011.

A. Bunse-Gerstner. Computational solution of the algebraic riccati equation. *Journal of The Society of Instrument and Control Engineers*, 35(8):632–639, 1996.

V. V. Dombrovskii and E. A. Lyashenko. A linear quadratic control for discrete systems with random parameters and multiplicative noise and its application to investment portfolio optimization. *Automation and remote control*, 64(10):1558–1570, 2003.

N. Elia. Remote stabilization over fading channels. *Systems Control Letters*, 54(3):237–249, 2005.

F. Feitzinger, T. Hylla, and E. W. Sachs. Inexact kleinman-newton method for riccati equations. *SIAM Journal on Matrix Analysis and Applications*, 31(2):272–288, 2009.

Y. Feng, X. Chen, and G. X. Gu. Robust stabilization subject to structured uncertainties and mean power constraint. *Automatica*, 92:1–8, 2018a.

Y. Feng, X. Chen, and G. X. Gu. Multiobjective  $\mathcal{H}_2$  control design subject to multiplicative input dependent noises. *SIAM Journal on Control and Optimization*, 56(1):253–271, 2018b.

Harold Joseph H. J. Kushner. Stochastic stability and control. 1967.

D. Hinrichsen and A. J. Pritchard. Stability radii of systems with stochastic uncertainty and their optimization by output feedback. *SIAM Journal on Control and Optimization*, 34(6):1972–1998, 1996.

J. H. Hu, J. L. Shen, and D.H. Lee. Resilient stabilization of switched linear control systems against adversarial switching. *IEEE Transactions on Automatic Control*, PP:1–1, 01 2017.

J. H. Hu, J. L. Shen, and D. H. Lee. Optimal stabilizing rates of switched linear control systems under arbitrary known switchings. *Automatica*, 159:111331, 2024.

L. W. Jacques and C. W. Jan. Feedback stabilizability for stochastic systems with state and control dependent noise. *Automatica*, 12(3):277–283, 1976.

H. K. Khalil and J. W. Grizzle. *Nonlinear systems*, volume 3. Prentice hall Upper Saddle River, NJ, 2002.

D. Kleinman. On the stability of linear stochastic systems. *IEEE Transactions on Automatic Control*, 14(4):429–430, 1969.

A. Laub. A schur method for solving algebraic riccati equations. *IEEE Transactions on Automatic Control*, 24(6):913–921, 1979.

B. Lemmens and R. Nussbaum. *Nonlinear Perron-Frobenius Theory*, volume 189. Cambridge University Press, 2012.

L. Li, H. S. Zhang, and Y. Wang. Stabilization and optimal control of discrete-time systems with multiplicative noise and multiple input delays. *Systems Control Letters*, 147:104833, 2021.

J. B. Lu and R. E. Skelton. Mean-square small gain theorem for stochastic control: discrete-time case. *IEEE Transactions on Automatic Control*, 47(3):490–494, 2002.

P. McLane. Asymptotic stability of linear autonomous systems with state-dependent noise. *IEEE Transactions on Automatic Control*, 14(6):754–755, 1969.

Q. Nguyen and K. Sreenath. Exponential control barrier functions for enforcing high relative-degree safety-critical constraints. In *2016 American Control Conference (ACC)*, pages 322–328, 2016.

Y.-H. Ni, R. Elliott, and X. Li. Discrete-time mean-field stochastic linearquadratic optimal control problems, ii: Infinite horizon case. *Automatica*, 57:65–77, 2015.

R. Penrose. A generalized inverse for matrices. *Mathematical Proceedings of the Cambridge Philosophical Society*, 51(3):406413, 1955.

Q. Y. Qi and H. S. Zhang. Output feedback control and stabilization for multiplicative noise systems with intermittent observations. *IEEE Transactions on Cybernetics*, 48(7):2128–2138, 2018.

T. Qi, J. Chen, W. Z. Su, and M. Y. Fu. Control under stochastic multiplicative uncertainties: Part i, fundamental conditions of stabilizability. *IEEE Transactions on Automatic Control*, 62(3):1269–1284, 2017.

E. Weitenberg, C. De Persis, and N. Monshizadeh. Exponential convergence under distributed averaging integral frequency control. *Automatica*, 98:103–113, 2018.

J. Willems and G. Blankenship. Frequency domain stability criteria for stochastic systems. *IEEE Transactions on Automatic Control*, 16(4):292–299, 1971.

W. M. Wonham. Optimal stationary control of a linear system with state-dependent noise. *SIAM Journal on Control*, 5(3):486–500, 1967.

C. W. Yao, B. D. Hsu, and B. S. Chen. Constructing gene regulatory networks for long term photosynthetic light acclimation in arabidopsis thaliana. *BMC bioinformatics*, 12(1):335, 2011.

H. S. Zhang, L. Li, J. J. Xu, and M. Y. Fu. Linear quadratic regulation and stabilization of discrete-time systems with delay and multiplicative noise. *IEEE Transactions on Automatic Control*, 60(10):2599–2613, 2015.

Y. F. Zhang and J. Cortés. Distributed transient frequency control for power networks with stability and performance guarantees. *Automatica*, 105:274–285, 2019.